

Exploring a New Design Paradigm for Omnidirectional MAVs for Minimal Actuation and Internal Force Elimination: Theoretical Framework and Control

Ahmed Ali*, Chiara Gabellieri*, Antonio Franchi*,†

Abstract—This paper presents a novel concept for achieving omnidirectionality in a multirotor aerial vehicle (MAV) that uses only 6 inputs and ensures no internal forces at the equilibria. The concept integrates a single actively-tilting propeller along with 3 pendulum-like links, each carrying a propeller, connected by passive universal joints to the main body. We show that this design ensures omnidirectionality while minimizing the internal forces and without resorting to overactuation (i.e., more than 6 inputs). A detailed dynamic model of the multi-link MAV is first developed. Afterwards, the analysis identifies the equilibrium configurations and illustrates that a forced equilibrium exists for every pose of the MAV’s main platform. In order to render this equilibrium asymptotically stable for the closed-loop system, a geometric nonlinear controller is constructed using dynamic feedback linearization and backstepping techniques with the main platform configuration error being the left-trivialized error on $SE(3)$. The stability of the closed-loop system is then investigated by employing standard Lyapunov arguments on the zero dynamics. We conclude by providing numerical simulations validating the proposed approach. They demonstrate the MAV capability to perform decoupled attitude and translational motions under non-zero initial conditions, parametric uncertainty, and actuators noise.

I. INTRODUCTION

Nowadays, Multirotor Aerial Vehicles (MAVs) are widely used in a variety of applications, ranging from agriculture to civil engineering [1]. Interest in this technology is growing, geared by its potential to perform tasks that require physical interaction with environments inaccessible to other types of mobile vehicles [2], [3]. While conventional quadrotors can efficiently handle some of these tasks, particularly when special orientation maneuvers are not required, certain applications have emerged in which the capability of executing decoupled translational and rotational motions is essential, necessitating the demand for new MAV designs since quadrotor dynamics inherently prohibits this kind of motion. One notable example where the MAV platform needs to maintain constant orientation while translating in space is the contact-based inspection of sloped surfaces [4], [5].

* Robotics and Mechatronics Department, Electrical Engineering, Mathematics, and Computer Science (EEMCS) Faculty, University of Twente, 7500 AE Enschede, The Netherlands. ahmed.ali@utwente.nl, c.gabellieri@utwente.nl, a.franchi@utwente.nl

†Department of Computer, Control and Management Engineering, Sapienza University of Rome, 00185 Rome, Italy. antonio.franchi@uniroma1.it

This work was partially funded by the Horizon Europe research agreement no. 101120732 (AUTOASSESS).

A. Research Problems and Related Work

When designing a new MAV, one can easily be convinced that it is desirable to obtain all the angular velocities of the propellers aligned with each other and with the gravity force at any static hovering equilibrium: this avoids internal propeller-generated forces canceling each other at the cost of a higher energy consumption; moreover, it is desirable to keep the number of actuators to the minimum (equal to the task dimension), to reduce the payload (which, in turn, affects the vehicle’s endurance), the cost, the maintenance requirements, etc. Furthermore, for tasks requiring high dexterity like the ones mentioned before, it is desirable for the MAV to be able to statically hover at any pose (in $SE(3)$ in general). Last but not least, the design of a MAV must also allow the controlled stabilization of its hovering equilibria. We label these four desirable properties as the Internal-force Property, the Input-dimension Property, the Equilibria Property, and the Stabilizability Property, respectively.

When restricting the problem to the vertical 2D space, we demonstrated in [6] that a MAV design with all the above four properties exists. Especially, it can be stabilized at any static equilibrium pose in $SE(2)$ with propellers parallel to each other and the gravity vector, and it has only three actuators. The actuators are two brushless motors attached to one propeller each and one servomotor that actively tilts one of the two propellers, while the other one is free to passively rotate and has a center of mass not coincident with the rotation point. However, extending such a result to the 3D space is very far from being trivial and is an open problem. Just to mention two obstacles to such extension: $SE(3)$ is a fundamentally different manifold than $SE(2)$ and the dynamic effects related to single revolute joints in 2D cannot be extended to the case of multiple joints in 3D, see model in Sec. II-B. Moreover, in the 3D space, the propeller drag torques arise and have to be taken into account, see discussion in Sec. III-A.

We will now revise the main MAV designs proposed in the literature and show that none of them has all the four desirable properties described above.

Standard underactuated MAVs like quadrotors and hexarotors tick the Internal-force Property as they have all propellers fixedly oriented with spinning axes parallel to each other; however, because of the fixed attachment between the propellers and the body frame, their only hovering equilibria

are characterized by the attitudes where the z axis is aligned with the gravity vector. Thus, they do not tick the Equilibria property.

Aerial vehicles equipped with the ability to hover while maintaining a larger set of orientations, known as fully-actuated MAVs, are surveyed in [7]. These MAVs cannot be stabilized at any pose but at a subset of poses in $SE(3)$ determined by the thrust limits, the design kinematics, and joint limits. Such subset contains any position but only a subset of all the orientations in general. A subclass of this type of MAVs, called omnidirectional MAV [8], can hover at any pose: namely, they have the Equilibria property mentioned above. These aerial vehicles can be divided in two classes.

The first class of designs that have been proposed to achieve full actuation or omnidirectionality are realized by fixedly tilting the propellers in such a way that their spinning axes are not all parallel to each other. As a consequence, all of these designs do not have the Internal-force Property. Examples are [9], a fully actuated hexarotor, and [10], [11], omnidirectional hexarotors. Other omnidirectional fixedly-tilted-propeller designs do not comply with the Input-dimension Property, either; they are, for example, the heptarotor presented in [12] or the octarotors proposed in [13], [14].

The second design approach to achieve full-actuation or omnidirectionality while also partially achieving the Internal-force Property for at least some hovering orientations is the addition of servomotors that actively change the relative orientation between the propellers and the frame of the MAV. In [15], [16], the authors present a modification of the conventional quadrotor by actuating the tilt of each propeller separately via 4 servomotors for a total of 8 actuators. Similarly, in [17], the authors used 6 servomotors in addition to the 6 brushless motors that rotate the 6 propellers of an hexarotor. The design in [18] also falls in this category. They developed a MAV with multiple links connected in series by active revolute joints, with each link having two propellers that rotate simultaneously using a motor. In an attempt to limit the number of actuators, some designs have been proposed in which a single servo-motor is used to synchronously tilt all the propellers: 6 propellers are synchronously tilted by the additional actuator in [19], and 8 propellers in [20]. All the aforementioned designs do not comply with the Input-dimension Property, having a number of actuators greater than 6. Furthermore they do not comply with the Internal-force Property at any orientation but only some at some specific ones.

B. Contributions

The main contribution of this work is to propose the first MAV design, to the best of the authors' knowledge, having the following properties in $SE(3)$.

- 1) Input-dimension property. The number of actuators in the proposed MAV design is 6, equal to the number of DoFs of its base's pose. There are 4 brushless motors, each making one propeller spin; 3 of the

propellers are connected to a passive 2-DoF joint; one of the propeller's attitude is actively controlled by 2 servomotors.

- 2) Equilibria property. In Proposition 1, we show that static hovering is feasible at *any* pose in $SE(3)$ of the MAV's main body; in other words, a forced equilibrium exists for any base's pose.
- 3) Internal-force property. Proposition 1 also shows that no internal forces are produced at the equilibrium for any base pose in $SE(3)$.
- 4) Stabilizability property. We prove in Theorem 1 that it is possible to create a geometric state feedback law that renders the closed-loop system of the MAV asymptotically stable at any base pose in $SE(3)$, as long as configuration and thrust trajectories of the system remain in a certain neighborhood of that base pose. We observe that the dynamics of the passive propeller joints coincide with the zero dynamics, and we prove its asymptotical stability using the Lyapunov theory. The feedback control law is given in Proposition 2.

Eventually, simulation results of the closed-loop system in the presence of non-idealities, such as noise and parameter uncertainties, are presented, in order to provide an acceptable level of confidence in the generalizability of the result beyond the standard model used to formally prove all the properties.

C. Motivations Behind the Design Idea

The simplest MAV design that one could think of that respects the Input-dimension Property and the Internal-force Property (and potentially the Equilibria Property) is the one with 6 propellers, all free to passively tilt like 3D pendulums. However, the results achieved for the 2D example in [6] showed that a design with 3 passively linked propellers in a pendulum like fashion, in that case, was non-feedback linearizable as the allocation matrix was structurally rank-deficient at the static equilibria. Based on such a preliminary result, we discarded the all-passive-propeller design.

Hence, our design has servomotors that actively reorient one propeller. An alternative could be to reorient actively *all* the four propellers synchronously by means of the two servomotors and a transmission mechanism. However, the design of such a mechanism to drive the whole propeller joints synchronously is not trivial, would bring mechanical complexity and with it additional payload, cost, and maintenance effort; furthermore, it would not scale well with the size of the vehicle, when the motion needs to be transferred over longer distances. Instead, the proposed design where the servomotors exert their actuation locally at one individual propeller has the advantage of being modular and simple from a mechanical point of view, not posing challenges when increasing the dimensions of the vehicle.

D. Outline

The rest of the paper is organized as follows. Sec. II describes the dynamic model of the proposed novel MAV conceptual idea, whereas Sec. III identifies the equilibria sets of that model being all the poses in $SE(3)$ and all having

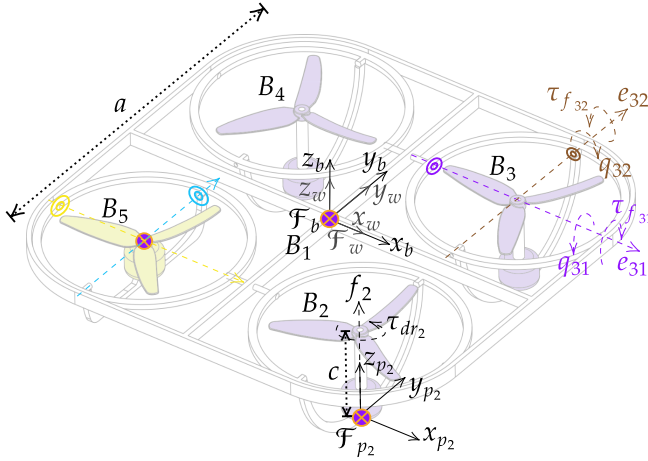


Fig. 1: Conceptual representation of the proposed MAV idea. The origins of the frames \mathcal{F}_b and \mathcal{F}_{p_2} are attached to CoMs of the base B_1 and the propeller link B_2 , respectively. The shown configuration is when \mathcal{F}_b coincides with \mathcal{F}_w and all the frames of the links have the same orientation as \mathcal{F}_w . The joint q_{j1} and q_{j2} positions are zero when \mathcal{F}_{p_j} has the same orientation as \mathcal{F}_b , $j = \{2, \dots, 5\}$. The link B_5 is attached to B_1 through an active joint, unlike the rest of the joints which are passive.

the internal force property. Afterwards, we investigate and demonstrate that the system can be made asymptotically stable at all these equilibria by a state feedback in Sec. IV. Numerical simulations where the MAV performs decoupled motions are the subject of Sec. V. We conclude by giving some remarks on the future work in Sec. VI. For ease of exposition, all the formal proofs are collected in a separate section: Sec. VII.

II. PROPOSED DESIGN AND DYNAMICAL MODEL

In this section, we describe the proposed design and derive its dynamical model in state-space representation.

A. Mechanical Design Idea

The vehicle concept, depicted in Fig. 1, is composed of a main rigid body called the *base* and denoted with B_1 , and four smaller bodies, referred to as *links* and denoted with B_2, B_3, B_4 and B_5 . Each link is connected to the base by means of two revolute joints, thoroughly described in the following, and hosts a rigidly attached velocity controlled brushless (BL) motor driving a propeller. We refer as the *actuation unit* to each sub-system composed by the propeller, the BL motor, the link, and the two revolute joints connecting the link with the base, for a total of four actuation units. The rotation axes of the two revolute joints of each actuation unit are assumed to intersect in one point, called the *center of rotation* of the corresponding link, which also coincides with the center of the propeller.

The CoM's of B_2, B_3 , and B_4 are located substantially below their centers of rotation. This can be achieved for example by lowering enough the position of the BL motors of these actuation units, which typically are the heaviest parts. This design makes the three links resemble three spatial pendula with the corresponding joints acting as their pivots.

The CoM of B_5 is instead assumed to be coincident with its center of rotation, for a reason that will be clear in the following.

The actuation units are mounted on the base in such a way that their centers of rotation (i.e., the propeller thrust application points) are all placed on the same plane. This is referred to as a *coplanar design*.

The two revolute joints connecting B_5 with B_1 are assumed to be actuated by two servomotors, representing together a universal joint denoted with J_{15} , whose configuration is denoted with $q_5 \in \mathbb{T}^2$. The six revolute joints connecting B_1 with B_2, B_3 , and B_4 , are *passive*, representing three universal joints denoted with J_{12}, J_{13} , and J_{14} , respectively, whose configurations are denoted with $(q_2, q_3, q_4) \in \mathbb{T}^6$.

For what has been said so far, the generic universal joint J_{1j} , with $j = 2, \dots, 5$, is then constituted by two consecutive 1-DoF mutually-orthogonal revolute joints whose configurations are represented by $q_{j1} \in \mathbb{S}^1$ and $q_{j2} \in \mathbb{S}^1$. We assign body-fixed reference frames to B_1, B_2, \dots, B_5 with origins coincident with the corresponding CoM's, and we denote them with $\mathcal{F}_b, \mathcal{F}_{p_2}, \mathcal{F}_{p_3}, \mathcal{F}_{p_4}$ and \mathcal{F}_{p_5} respectively. The rotational axes corresponding to q_{j1} and q_{j2} are given by the unit vectors, expressed in frame \mathcal{F}_b , $e_{j1} = (1 \ 0 \ 0)^T$ and $e_{j2} = R_{x_b}(q_{j1})(0 \ 1 \ 0)^T$, respectively, where $R_k(*)$ is a pure rotation around axis k by the angle $*$. Moreover, we assume that each joint composing the passive universal joint J_{1j} , with $j = 2, 3, 4$, has viscous friction torques applied about e_{j1} and e_{j2} and symbolized by $\tau_{f_{j1}}$ and $\tau_{f_{j2}}$, respectively.

For the sake of model simplicity, the actuated joint J_{15} is assumed to be driven by two fast servo DC motors taking the joint velocity $u_v \in \mathbb{R}^2$ as a control input. The motor dynamics is assumed negligible. Furthermore, to improve the formal tractability of the model, we assume that the mass distribution of B_5 is concentrated at its CoM point which is coincident with its center of rotation. Under such convenient assumptions, the angular moment of inertia of link B_5 referred to \mathcal{F}_{p_5} is zero. This causes the dynamics of the link B_5 projected onto the minimal coordinates q_5 to be exactly zero due to the fact that both the time rate of change of the body momentum along with the gravitational wrench vanish when mapped through the screw encoding the kinematical constraints between B_1 and B_5 . Therefore, the dynamics of q_5 is solely governed by the motor rotational speed, i.e., $\dot{q}_5 = u_v$.

We differentiate between two types of Passive Joints Designs (PJD), denoted in the following as PJD₁ and PJD₂, respectively. The design PJD₁ has no additional feature with respect to the one described so far, whereas the design PJD₂ includes an additional Pulley-Belt-Spring module as illustrated in Fig. 2. This schematic shows a pulley (p_{j1}) transferring the rotation around the axis \bar{y}_{p_j} , attached to the link B_j , with $j = 2, 3, 4$, by an amount of q_{j2} , to equivalent rotation around the axis \bar{x}_b , attached to the intermediate link \bar{B}_j , through the belt (b) and pulley (p_{j2}). The torsion spring (s), wound along the axis \bar{x}_b , is connected to the pulley (p_{j2}) such that it compresses with the rotation of this pulley. The

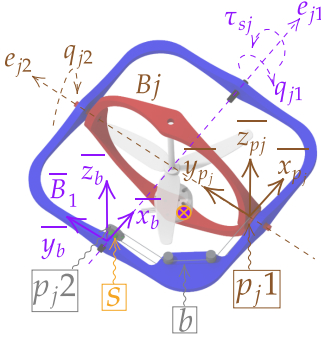


Fig. 2: The connection between B_j ($j = 2, 3, 4$) and the base B_1 in PJD₂ consists of universal passive joint with a Pulley-Belt-Spring module. \bar{B}_j is the intermediate link connecting B_1 to B_j . b , p and s denote the belt, pulley and a torsion spring, respectively. τ_{sj} is the torsion spring torque around the rotation axis of q_{j1} , i.e. e_{j1} .

spring is fixed at the other end to a point in \bar{B}_j .

The spring thus applies a moment to the link \bar{B}_j around \bar{x}_b that is a function of q_{j2} . The entire structure of PJD₂ moves with \bar{B}_j , hence the rotation of joint q_{j1} between B_1 and \bar{B}_j has no effect on the operation of the Pulley-Belt-Spring module whatsoever. In other words, the mechanism is unidirectional, meaning that rotation of B_j around e_{j2} causes a moment applied to \bar{B}_j around e_{j1} while the reverse is not true due to the module being fixed in place w.r.t \bar{B}_j and housed in it. The rationale behind introducing PJD₂ and how the spring is tuned shall become clear in Sec III-A. The analysis presented herein applies to both cases, unless stated otherwise explicitly.

B. Equations of Motion

We denote with $\mathcal{Q} = (x_1, q_5) \in SE(3) \times \mathbb{T}^8$ the configuration of the whole system, where $x_1 \in SE(3) \times \mathbb{T}^6$ is defined as

$$x_1 = \begin{pmatrix} x_{11} \\ x_{12} \end{pmatrix} := \begin{pmatrix} C_1^0 \\ q_t \end{pmatrix} \quad (1)$$

where $x_{11} := C_1^0 \in SE(3)$ is the configuration of the base B_1 relative to the inertial world frame \mathcal{F}_w whereas $x_{12} := q_t = (q_2, q_3, q_4) \in \mathbb{T}^6$. The velocity of $x_1(t)$ is denoted by $x_2 \in se(3) \times \mathbb{R}^6$ which is given as

$$x_2 := \begin{pmatrix} x_{21} \\ x_{22} \end{pmatrix} = \begin{pmatrix} V_1^0 \\ \dot{q}_t \end{pmatrix} \quad (2)$$

where $x_{21} := V_1^0 = \dot{C}_1^0(C_1^0)^{-1} \in se(3)$ represents the right differential on $SE(3)$, or equivalently, the right invariant (spatial) twist of the base B_1 relative to, and expressed in, the inertial world frame \mathcal{F}_w , while $x_{22} := \dot{q}_t = (\dot{q}_2, \dot{q}_3, \dot{q}_4) \in \mathbb{R}^6$ are the joint speeds of the passive joints.

The motion is then described by the dynamical equations

$$M(x_1)\dot{x}_2 + h(x_1, x_2) + \bar{g}(x_1) - \bar{\tau}_f(x_{22}) = W_{app}^0(x_1) \quad (3)$$

$$\dot{q}_5 = u_v$$

where the meaning of all the symbols not yet defined and appearing in (3) are provided in Table I with $j = 2, 3, 4$ and $i = 1, 2$.

Denote the full state vector $x(t)$ as $x = (x_1, x_2, q_5)^T \in \mathbb{X} \equiv SE(3) \times \mathbb{T}^8 \times se(3) \times \mathbb{R}^6$. Then (3) can be put in the state space form Σ_1 as follows

$$\Sigma_1 : \begin{cases} \dot{x} = \begin{pmatrix} [x_{21}] x_{11} \\ x_{22} \\ M^{-1}(-h - g + \bar{\tau}_f) \\ 0_{2 \times 1} \end{pmatrix} \\ \begin{pmatrix} 0_{12 \times 6} & 0_{6 \times 2} \\ D_b & 0_{6 \times 3} \\ D_t & I_{2 \times 2} \end{pmatrix} u \end{cases} \quad (4)$$

where $[\cdot]$ denotes the matrix form of $se(3)$, and D_b , D_t and the input vector u are defined as

$$D_b = \begin{pmatrix} \text{Ad}_{(C_{f_2}^0)^{-1}}^T \bar{f}_2 & \text{Ad}_{(C_{f_3}^0)^{-1}}^T \bar{f}_3 & \text{Ad}_{(C_{f_4}^0)^{-1}}^T \bar{f}_4 & \text{Ad}_{(C_{f_5}^0)^{-1}}^T \bar{f}_5 \end{pmatrix}_{6 \times 4}$$

$$D_t = \begin{pmatrix} S_2^T \text{Ad}_{(C_{f_2}^0)^{-1}}^T \bar{f}_2 & 0 & 0 \\ 0 & S_3^T \text{Ad}_{(C_{f_3}^0)^{-1}}^T \bar{f}_3 & 0 \\ 0 & 0 & S_4^T \text{Ad}_{(C_{f_4}^0)^{-1}}^T \bar{f}_4 \end{pmatrix}_{6 \times 3}$$

$$u = (f_2 \ f_3 \ f_4 \ f_5 \ u_{v_1} \ u_{v_2})_{6 \times 1}^T \in \mathbb{R}^6$$

where $f = \text{col}(f_i)$ and f_i is the thrust magnitude of the propeller attached to B_i , with $i = 2, \dots, 5$; f_i is a constant vector given as $\bar{f}_i := (0 \ 0 \ k_i \ 0 \ 0 \ 1)_{6 \times 1}^T$ with $k_i = \pm c_{d_i}/c_{f_i}$ representing the ratio between the drag and thrust coefficients c_{d_i} and c_{f_i} of link B_i 's propeller, respectively, see, e.g., [21]. $C_{f_i}^0 \in SE(3)$ is the homogeneous transformation of a frame \mathcal{F}_{f_i} attached at the propeller of link B_i relative to the inertial frame \mathcal{F}_w . Lastly, $\text{Ad}_{C_{f_i}^0} : SE(3) \rightarrow \text{GL}(6, \mathbb{R})$ is the adjoint action of the Lie group $SE(3)$ on its Lie algebra $se(3)$ and is computed by $\text{Ad}_C = \begin{pmatrix} R & 0 \\ [p]R & R \end{pmatrix}$, where R and p are the rotation matrix and position vector

Symbol	Definition	Formula
q_j	Joint J_{1j} 's configuration	$q_j = \text{col}(q_{ji}) \in \mathbb{T}^2$
q_t	Passive joints configuration	$q_t = \text{col}(q_j) \in \mathbb{T}^6$
S_j	Joint J_{1j} 's spatial instantaneous screw	$S_j = (S_{j1} \ S_{j2})$, with $S_{ji} \in se(3)$
S_t	Passive joints spatial instantaneous screw list	$S_t = \text{blockdiag}(S_j)$
M	Generalized mass matrix	$M = \begin{pmatrix} M_{bb} & M_{bt} \\ M_{tb}^T & M_{tt} \end{pmatrix}$
M_{bb}	Generalized base B_1 mass matrix	$M_{bb} = M_{B_1}^0 + \sum_{j=2}^5 M_{B_j}^0$, with $M_{B_j}^0$ being B_j 's inertia tensor referred to the world frame \mathcal{F}_w
M_{bt}	Generalized coupling mass matrix	$M_{bt} = \sum_{j=2}^4 M_{B_j}^0 S_j$
M_{tt}	Generalized joint mass matrix	$M_{tt} = \text{blockdiag}(S_j^T M_{B_j}^0, S_j)$
\dot{M}_j^0	Time derivative of B_j 's inertia tensor referred to the world frame \mathcal{F}_w	$\dot{M}_j^0 = -M_j^0 \text{ad}_{V_1^0} - \text{ad}_{V_1^0}^T M_j^0$, with $\text{ad}_{V_j^0}$ denoting the adjoint operator on V_j^0 (the spatial twist of body B_j), $V_j^0 = V_1^0 + S_j \dot{q}_j \forall j \in \{2, 3, 4\}$. Also, $M_5^0 = -M_5^0 \text{ad}_{V_1^0} - \text{ad}_{V_1^0}^T M_5^0$.
\dot{S}_j	Time derivative of screw S_j	$\dot{S}_j = \text{ad}_{V_j^0} S_j$
h	Coriolis & centrifugal terms	$h = (h_b \ \text{col}(h_j))^T$
h_b	Base B_1 Coriolis & centrifugal terms	$h_b = M_{bb} V_1^0 + \sum_{j=2}^4 (M_{B_j}^0 \dot{S}_j + \dot{M}_{B_j}^0 S_j) \dot{q}_j$
h_j	B_j 's Coriolis & centrifugal terms projected onto joint J_{1j}	$h_j = S_j^T ((M_{B_j}^0 \dot{S}_j + \dot{M}_{B_j}^0 S_j) \dot{q}_j + \dot{M}_{B_j}^0 V_j^0)$
W_{grav, B_j}^0	Spatial gravitational wrench applied at B_j 's CoM	$W_{grav, B_j}^0 = M_{B_j}^0 G^0$, with $G^0 = \text{col}(0_5, -g)$. Here \dot{g} is the gravity acceleration.
\bar{g}	Gravitational terms	$\bar{g} = (g_b \ g_t)^T$
g_b	Base B_1 gravitational force	$g_b = -\sum_{j=1}^5 W_{grav, B_j}^0$
g_t	Joint gravitational torque	$g_t = -S_t^T \text{col}(W_{grav, B_j}^0)$
$W_{app, b}^0$	Applied external spatial wrench at base B_1 's CoM	$W_{app, b}^0 = \sum_{j=2}^5 W_{app, B_j}^0 \in se(3)^*$, with $W_{app, B_j}^0 \in se(3)^*$ being the applied spatial wrench at B_j 's CoM
$W_{app, t}^0$	Applied external spatial wrench at pendulum links B_2, B_3, B_4 projected onto the respective joints through S_t	$W_{app, t}^0 = S_t^T \text{col}(W_{app, B_j}^0)$
W_{app}^0	Total applied external wrenches	$W_{app}^0 = (W_{app, b}^0 \ W_{app, t}^0)^T$
τ_{fj}	Joint J_{1j} 's applied viscous friction torque	$\tau_{fj} = \text{col}(\tau_{fj_i}) \in \mathbb{R}^2$, and $\bar{\tau}_f = (0_{6 \times 1} \ \text{col}(\tau_{fj}))^T$

TABLE I: Variable definitions and formulas

of C , respectively.

Result 1 (Input dimension property). *The proposed design satisfies the input dimension property. In fact the dimension of the manifold of the configuration of the base frame C_1^0 is six and the dimension of the input is $\dim(u) = 6$ (four propeller speeds and two servomotor speeds). In other words, the system is square with respect to the output being C_1^0 , the pose of B_1 .*

III. STUDY OF ATTAINABLE EQUILIBRIA AND INTERNAL FORCES AT EACH EQUILIBRIUM

In this section we obtain the set of forced equilibria of the dynamics (4) and investigate their properties in terms of the corresponding four thrust forces produced at these configurations. We begin by giving some preliminary definitions. Afterwards, the main result is summarized in Proposition 1 whose proof is found in Sec. VII-B.

The value of a variable at an equilibrium is identified by a subscript e . Imposing $\dot{x}(t) = 0$ in (4) implies $(x_2(t), \dot{q}_5(t)) = 0$, which defines an equilibrium condition at which the state and the input become, respectively, $x_e = (x_{1e}, 0, q_{5e})^T$ and $u_e = (f_e \ u_{ve})^T$ with $f_e = (f_{2e} \ f_{3e} \ f_{4e} \ f_{5e})^T$ and $u_{ve} = (u_{v1e} \ u_{v2e})^T$. This condition yields $h(x_1(t), x_2(t)) = 0$ since it depends quadratically on the configuration velocity state $x_2(t)$, as apparent from Table I. Similarly, the viscous friction $\bar{\tau}_f(x_{22}(t)) = 0$. For PJD₁, this reduces (4) to this static balance vector equation whose admissible solutions are the equilibrium state and input pairs (x_e, u_e) such that

$$g_b(C_{1e}^0, q_{te}) = W_{app,b}^0(f_e, q_{te}, q_{5e}), \quad (6)$$

$$g_t(C_{1e}^0, q_{te}) = W_{app,t}^0(q_{te}, f_{2e}, f_{3e}, f_{4e}) := (D_t \ 0_{6 \times 3}) u_e \\ = (\tau_{d2} \ 0 \ \tau_{d3} \ 0 \ \tau_{d4} \ 0)_{6 \times 1}^T, \quad 0_2 = u_{ve} \quad (7)$$

where $\tau_{dj} = k_j f_{je} \sin(q_{j2e})$ – with $j = 2, 3, 4$ – represents the drag component of the propeller of B_j factorized on the axis e_{j1} of the joint variable q_{j1} at an equilibrium; C_{1e}^0 and $q_{te} = \text{col}(q_{je})$, with $q_{je} = \text{col}(q_{jie}) \forall j = 2, 3, 4$ and $\forall i = 1, 2$, symbolizing an equilibrium of the base configuration C_1^0 and the passive joints configuration q_t , respectively.

A. Effect of the Aerodynamic Drag Torque at the Equilibrium

The presence of the torque τ_{dj} in (7) leads to the important consequence that the value of the joints q_{te} at the equilibrium is not solely determined by the gravitational torque at equilibrium g_{te} , as it is the case for the 2D MAV presented in [6], but also by a component of the equilibrium thrust f_e at equilibrium.

This residual torque can be eliminated at any equilibrium by the spring introduced in PJD₂. In fact, we can tune each torsion spring to have a variable stiffness $k_s := \frac{\partial \tau_{sj}}{\partial q_{j2}} = k_j f_{je} \cos(q_{j2})$ where τ_{sj} is the torque absorbed by the spring at the joint angle q_{j2} . This task is facilitated by the fact that the term $k_j f_{je}$ is always constant since f_{je} is found to be constant for any equilibrium of PJD₂, as proven in Sec. VII-B (49). As a result, this component τ_{dj} is canceled at any

PJD₂ equilibrium, i.e., $\tau_{dj} = -\tau_{sje}$, transforming (7) to

$$g_t(C_{1e}^0, q_{te}) = 0_6, \quad u_{ve} = 0_2. \quad (8)$$

We solve (7) and (8) in Sec. VII-B for the joint equilibrium q_{je} . To distinguish between a joint equilibrium of PJD₁ and PJD₂, let $q_{te}^{[i]}$ denote a joint equilibrium solution of PJD_i, with $i = 1, 2$, and $f_e^{[i]}$ be the associated thrust, respectively.

B. Minimal Thrust at Equilibrium vs Presence of Internal Forces

Before presenting the result on the equilibria property of the proposed MAV (4) we provide two definition for the thrust magnitudes at the equilibrium, in the case in which they are minimal and in the case in which there is internal force.

Definition 1. A vector of thrust magnitudes $f \in \mathbb{R}_{\geq 0}^l$, where $\mathbb{R}_{\geq 0}^l := \{s = \text{col}(s_i) \in \mathbb{R}^l \mid s_i \geq 0, \forall i \in \{1, \dots, l\}\}$, is said to be minimal at the equilibrium if it belongs to $\mathcal{F}_{\min}^{\text{eq}}$, defined as:

$$\mathcal{F}_{\min}^{\text{eq}} := \left\{ f = \text{col}(f_i) \in \mathbb{R}_{\geq 0}^l \mid \sum_{i=1}^l f_i = m_{\text{tot}} g \right\} \quad (9)$$

where m_{tot} is the total mass of the system. Instead, f is said to have internal forces at the equilibrium if it belongs to $\mathcal{F}_{\text{int.for.}}^{\text{eq}}$, defined as:

$$\mathcal{F}_{\text{int.for.}}^{\text{eq}} := \left\{ f = \text{col}(f_i) \in \mathbb{R}_{\geq 0}^l \mid \sum_{i=1}^l f_i > m_{\text{tot}} g \right\} \quad (10)$$

A MAV design whose thrust magnitudes are minimal at all its equilibria is said to have no internal forces at its equilibria.

In other words, a minimal thrust magnitudes vector $f \in \mathcal{F}_{\min}^{\text{eq}}$ has the least amount of total thrust magnitudes necessary to counteract the gravity effect at the equilibrium, whereas $f \in \mathcal{F}_{\text{int.for.}}^{\text{eq}}$ means that the vehicle generates more total thrust than what is strictly necessary for compensating gravity, thus having some wasted internal force.

Moreover, there exists a unique orientation for each propeller in the system such that when all the propellers assume such orientation the absence of internal force is guaranteed at hovering. The following lemma provides the formal statement.

Lemma 1. Consider a vehicle with a thrust magnitudes vector $f = \text{col}(f_i) \in \mathbb{R}_{\geq 0}^l$ with the corresponding propellers configurations $C_i^0(C_1^0, \alpha_i) \in \text{SE}(3)$, relative to a right-handed inertial frame whose z -axis direction opposes the axis along which the gravitational force is applied, where $C_1^0 \in \text{SE}(3)$ is the base configuration and $\alpha_i \in \mathbb{S}^2$ is the unit direction vector of the propeller i expressed in the inertial frame. At any equilibrium for the MAV with a given \bar{C}_1^0 , there is no internal force generated at such equilibrium if and only if all propellers, whose thrust magnitudes are $f_i > 0$, are pointing in the direction of inertial frame's z -axis, i.e. $C_i^0(\bar{C}_1^0, \alpha_i) e_3 = e_3 \ \forall i \in \{1, \dots, l\}$ with $e_3 = (0 \ 0 \ 1 \ 0)^T$.

Proof. See Sec. VII-A. \square

The following proposition establishes the main result of this section.

Proposition 1. Consider any pose for the base B_1 denoted by C_{1e}^0 . Then the following statements hold true and are equivalent for the system (4):

- 1) For any base pose $C_1^0 \in SE(3)$, there exists an equilibrium for PJD_2 in which the joint equilibrium configuration $q_{te}^{[2]}$ satisfies $C_j^0(C_{1e}^0, q_{je}^{[2]})e_3 = e_3 \forall j \in \{2, \dots, 5\}$ and a thrust magnitudes vector $f_e^{[2]} \in \mathcal{F}_{\min}^{\text{eq}}$ is produced whose elements are constant $\forall C_1^0$ and equal to (49).
- 2) For any base pose C_1^0 , PJD_2 has no internal force at any equilibrium $q_{te}^{[2]}$, by Definition 1, as a corollary of $f_e^{[2]} \in \mathcal{F}_{\min}^{\text{eq}}$ (Statement 1).
- 3) When $\tau_{dj} \neq 0$, PJD_1 has no joint equilibrium in which each propeller produces a minimal thrust: $C_j^0(C_{1e}^0, q_{je}^{[1]})e_3 \neq e_3, \forall \tau_{dj} \neq 0$.
- 4) When $\tau_{dj} \neq 0$, it follows from Statement 3 and Lemma 1 that PJD_1 has an internal force $f_e^{[1]} \in \mathcal{F}_{\text{int.for.}}^{\text{eq}}$. The amount of internal force changes with the parameters k_i, c and m_p , defined in Table II.

Proof. See Sec. VII-B. \square

The state equilibria sets for PJD_1 and PJD_2 can thus be defined as $\mathbb{D}_{x_e}^{[1]}$ and $\mathbb{D}_{x_e}^{[2]}$, respectively, with $i = 1, 2$

$$\begin{aligned} \mathbb{D}_{x_e}^{[i]} = & \left\{ x(t) \in \mathbb{X}, \{t, \bar{t}\} \in \mathbb{R}_{\geq 0} \mid \forall C_{1e}^0 \in SE(3), \forall t \geq \bar{t}, \right. \\ & x(t) := (C_1^0(t), q_1(t), x_2(t), q_5(t))^T \\ & = (C_{1e}^0(\bar{t}), q_{te}^{[i]}(\bar{t}), 0_{12}, q_{5e}^{[i]}(\bar{t})), \\ & \left. q_{te}^{[i]} \text{ from (54) or (42), for } i = 1, 2, \text{ respectively} \right\} \end{aligned} \quad (11)$$

while the associated thrust equilibrium sets are given by

$$\begin{aligned} \mathbb{D}_{f_e}^{[i]} = & \left\{ f(t) \in \mathbb{R}^4, \{t, \bar{t}\} \in \mathbb{R}_{\geq 0} \mid \forall t \geq \bar{t}, f(t) = f_e^{[i]}(\bar{t}), \right. \\ & f_e^{[i]} \text{ from (54) or (49), for } i = 1, 2, \text{ respectively} \left. \right\} \end{aligned} \quad (12)$$

We conclude the section remarking that the perfect vertical alignment of propellers in any PJD_2 equilibrium is possible thanks to each spring torque τ_{sje} absorbing the residual drag τ_{dj} affecting the joint variable q_{j1} . This allows any joint equilibrium $q_{te}^{[2]}$ to be dictated only by the gravity acting on the CoMs of the pendulum-like links B_2 - B_4 , given that the pivots, i.e., the joints, are passive.

Remark 1. The design using PJD_1 's constitutes still an excellent compromise between mechanical simplicity and energy efficiency, with the ability to outperform the state of the art designs when it comes to the amount of internal force needed at the the equilibria. In fact, for typical values of the aerodynamic and kinematic parameters the difference in the amount of internal forces generated in PJD_1 design remains small compared to PJD_2 case, as it can be seen for example

in the simulations of Section V. This supports the viability of the concept from a mechanical perspective by using the simpler design PJD_1 , if one does not want to resort to the particular joint design in PJD_2 .

IV. STABILIZATION OF THE EQUILIBRIA

This section presents the solution of the problem of whether every equilibrium point in the set $\mathbb{D}_{x_e}^{[i]}$, given in (11), can be made closed-loop asymptotically stable, at least locally, by an action of a regular state feedback law. For clarity, we first provide an informal outline of the solution's derivation and establish necessary definitions, leading to the core findings stated in Theorem 1 and Proposition 2.

A. Informal Outline of the Solution

Denote with $\Sigma_i(x; u)$ a system Σ_i whose states and inputs are respectively x and u . The analysis departs by noticing that there exists no static state feedback control $u = \alpha(x)$ rendering the closed-loop system $\Sigma_1(x; \alpha(x))$ in (4) locally asymptotically stable (LAS) in an open neighborhood $\mathbb{U}_{x_e} \subseteq \mathbb{X}$ of an equilibrium $x_e \in \mathbb{D}_{x_e}^{[i]}$, since it turns out that Σ_1 does not possess a well-defined vector relative degree at any $x_e \in \mathbb{D}_{x_e}^{[i]}$ [22]. However, the goal of stabilizing this closed-loop system at x_e is still attainable by means of dynamic state feedback.

Towards this end, we first observe that Σ_1 in (4) can be decomposed into two subsystems

$$\Sigma_1 : \Sigma_2(x_{12}, x_2, q_5; u, x_{11}) \text{ and } \Sigma_3(x_{11}; x_{21}) \quad (13)$$

where Σ_2 is found to belong to the class of dynamically input/output feedback linearizable systems w.r.t an output taken from $V_1^0 =: x_{21}$. Second, by applying the dynamic extension algorithm [23] on Σ_2 , an extended system $\Sigma_2(\bar{x}; w, x_{11})$ results, where the extended state is $\bar{x} \in \bar{\mathbb{X}} \equiv \mathbb{T}^8 \times se(3) \times \mathbb{R}^{10}$ and $w \in \mathbb{R}^6$ is the new input for its input precompensator. For this extended system Σ_2 , we compute a local diffeomorphism $H(\bar{x}) : \mathbb{U}_{\bar{x}_e} \rightarrow \mathbb{U}_{\bar{x}_e}$, with a domain in $\mathbb{U}_{\bar{x}_e} \subseteq \bar{\mathbb{X}}$ of $\bar{x}_e \in \mathbb{D}_{x_e}^{[i]} \cup \mathbb{D}_{f_e}^{[i]}$ (12), transforming it into its normal form represented by $\Sigma_2^H(\zeta, \eta; w, x_{11})$.

This normal form $\Sigma_2^H(\bar{x}; w, x_{11})$ has a state $\bar{x} := (\zeta, \eta) \in \mathbb{U}_{\bar{x}_e} \subseteq \bar{\mathbb{X}} \equiv se(3) \times se(3) \times \mathbb{T}^6 \times \mathbb{R}^6$, where $\mathbb{U}_{\bar{x}_e}$ denotes an open neighborhood of $\bar{x}_e =: (\zeta_e, \eta_e) = H(\bar{x}_e)$. The normal form is a feedback interconnection between the dynamics of the I/O map $\Sigma_\zeta(\zeta; \eta, w, x_{11})$ and some internal dynamics $\Sigma_\eta(\eta; \zeta, x_{11})$. Σ_ζ can be feedback linearized, becoming $\Sigma_\zeta^w(\zeta; v)$, by an action of a *regular* static state feedback $w = \alpha_w(\bar{x}, x_{11}, v)$ with a domain in $\mathbb{U}_{\bar{x}_e} \times SE(3) \times se(3)$, where $v \in se(3)$ is a virtual input.

At this point, we return to the Σ_1 decomposition in (13). Let us denote with $\Sigma_3^H(x_{11}; \zeta)$ the system Σ_3 in (13) after the diffeomorphism H is applied and with $\Sigma_{\bar{\zeta}}(\bar{\zeta}; v)$ its composition with the feedback linearized system Σ_ζ^w , i.e. $\Sigma_{\bar{\zeta}}$ is given by

$$\Sigma_{\bar{\zeta}} : \Sigma_\zeta^w(\zeta; v) \text{ and } \Sigma_3^H(x_{11}; \zeta) \quad (14)$$

where $\bar{\zeta}$ denotes ζ extended with x_{11} . We can now conclude that if there exists a static state feedback $v = \alpha_v(\bar{\zeta})$ locally

asymptotically stabilizing $\Sigma_{\bar{\zeta}}$ at $\bar{\zeta}_e := (\zeta_e, x_{11e})$, then, from Theorem 10.3.1 in [22], the cascaded interconnection of the autonomous system $\Sigma_{\bar{\zeta}}(\bar{\zeta}; \alpha_v(\bar{\zeta}))$ and $\Sigma_{\eta}(\eta; \bar{\zeta})$ is guaranteed to be LAS in $\mathbb{U}_{\bar{x}_e} \times SE(3)$ of (\bar{x}_e, x_{11e}) , provided that the zero dynamics $\Sigma_{\eta}(\eta; 0)$ is LAS at η_e .

This means that, as long as trajectories of $\Sigma_{\bar{\zeta}}$ and Σ_{η} remain in $\mathbb{U}_{\bar{x}_e} \times SE(3)$, any base pose x_{11e} of the original system Σ_1 (4) can be made locally asymptotically stable by a dynamic state feedback.

B. Main Results

Theorem 1 formalizes this result while Proposition 2 provides the stabilizing feedback $v = \alpha_v(\bar{\zeta})$ whose construction details, drawing upon a backstepping strategy on $\Sigma_{\bar{\zeta}}$, are laid out in the proof in Sec. VII-D.

Theorem 1. *Let the original system Σ_1 (4) be decomposed as in (13) and define the system $\Sigma_3(x_{11}; x_{21})$ to be $\Sigma_3 : \dot{x}_{11} = [x_{21}] x_{11}$ while $\Sigma_2(x_{12}, x_2, q_5; u, x_{11})$ is*

$$\Sigma_2 : \begin{cases} \dot{x} = \begin{pmatrix} x_{22} \\ M^{-1}(-h - g + \bar{\tau}_f) \\ 0_{2 \times 1} \end{pmatrix} + \begin{pmatrix} 0_{6 \times 6} \\ D_b & 0_{6 \times 2} \\ D_t & 0_{6 \times 3} \\ 0_{2 \times 4} & I_{2 \times 2} \end{pmatrix} u \\ = F(x) + G(x)u \end{cases} \quad (15)$$

Then, these statements are true

- 1) Σ_2 is dynamically input/output feedback linearizable w.r.t the I/O pair (u, h_y) , in an open neighborhood $\mathbb{U}_{\bar{x}_e} \subseteq \bar{\mathbb{X}}$ of $\bar{x}_e \in \mathbb{D}_{\bar{x}_e}^{[i]} \cup \mathbb{D}_{f_e}^{[i]}$, where the output function $h_y(t) : t \rightarrow se(3)$ is $h_y(t) = V_1^0 =: x_{21}$. This is accomplished by the input precompensator

$$z(t) = \text{col}(z_i) := f(t) \in \mathbb{R}^4, \dot{z} = \bar{w} \in \mathbb{R}^4, i = 2, \dots, 5 \quad (16)$$

and the linearizing state feedback $w := (\bar{w}, u_{v_1}, u_{v_2})^T$,

$$w = D_2^{-1} M_b (-F_2 + v) \quad (17)$$

where $v \in se(3)$ is the virtual input, and F_2 , D_2 and M_b are given in (68), (61) and (66). This path-connected open neighborhood $\mathbb{U}_{\bar{x}_e}$ of \bar{x}_e is defined as

$$\mathbb{U}_{\bar{x}_e} = \left\{ \bar{x}(t) \in \bar{\mathbb{X}} \mid \det(D_2(\bar{x})) \neq 0 \right\} \quad (18)$$

- 2) For any base pose $x_{11} \in SE(3)$, The original system Σ_1 , extended with the precompensator (16), has locally, in $\mathbb{U}_{\bar{x}_e} \times SE(3)$, asymptotically stable (LAS) zero dynamics w.r.t the output h_y , iff $\forall \bar{x} \in \mathbb{Z}_x - \{\bar{x}_e\}$

$$\|\tilde{f}\| < \frac{1}{\|D_3(q_t - q_{te})\|} \lambda_{\min}(D_f) \|\dot{q}_t\| \quad (19)$$

where $\tilde{f} = \text{col}(f_i), i = 2, 3, 4$, \mathbb{Z}_x is a set defined in (77), D_3 is given in (71) and $D_f > 0 \in \mathbb{R}^{6 \times 6}$ contains the constant passive joints friction coefficients.

Proof. See Sec. VII-C □

Proposition 2. *Consider the virtual control input v given by*

$$v = \ddot{\zeta}_{1e} + \bar{K}_d(\dot{\zeta}_{1e} - \dot{V}_1^0) + \bar{K}_a(\zeta_{1e} - V_1^0) \quad (20)$$

where ζ_{1e} , $\dot{\zeta}_{1e}$, $\ddot{\zeta}_{1e} \in se(3)$ are respectively given in (92) and (104). \bar{K}_d and $\bar{K}_a \in \mathbb{R}^{6 \times 6}$ are positive definite diagonal gain matrices chosen such that to make $(A - BK)$ Hurwitz where

$$A = \begin{pmatrix} 0_{6 \times 6} & I_{6 \times 6} \\ 0_{6 \times 6} & 0_{6 \times 6} \end{pmatrix}, B = \begin{pmatrix} 0_{6 \times 6} \\ I_{6 \times 6} \end{pmatrix}, K = \begin{pmatrix} \bar{K}_a & \bar{K}_d \end{pmatrix} \quad (21)$$

Given the precompensator in (16) and the linearizing control law in (17), substituting v into (17) asymptotically stabilizes the extended system Σ_1 with (16) in the open neighborhood $\mathbb{U}_{\bar{x}_e} \times SE(3)$, where $\mathbb{U}_{\bar{x}_e} \subseteq \bar{\mathbb{X}}$ of $\bar{x}_e \in \mathbb{D}_{\bar{x}_e}^{[i]} \cup \mathbb{D}_{f_e}^{[i]}$ is given in (18).

Proof. See Sec. VII-D □

C. Efficient Implementation of the Controller

We introduce here a novel version of the Articulated-body Inertia Algorithm (ABA), originally derived in [24], which is modified to recursively obtain the acceleration $(\ddot{q}_t, \dot{V}_1^0)$ needed to implement the feedback linearizing law (17) (20) efficiently, instead of inverting the matrix M in (3).

For the system in Fig. 1, a modified ABA computes $(\ddot{q}_t, \dot{V}_1^0)$ executing the following computations for each $j = 2, 3, 4$

$$\begin{aligned} M_{j2}^A &= M_{B_j}^0 \\ \psi_{j2} &= (S_{j2}^T M_{j2}^A S_{j2})^{-1} \\ W_{j2}^A &= -\text{ad}_{V_{j2}^0}^T M_{B_j}^0 V_{j2}^0 - W_{app, B_j}^0 - W_{grav, B_j}^0 \\ M_{j1}^A &= M_{j2}^A - M_{j2}^A S_{j2} \psi_{j2} S_{j2}^T M_{j2}^A \\ \psi_{j1} &= (S_{j1}^T M_{j1}^A S_{j1})^{-1} \\ W_{j1}^A &= M_{j2}^A \left(S_{j2} \ddot{q}_{j2} + \dot{S}_{j2} \dot{q}_{j2} \right) + W_{j2}^A \end{aligned} \quad (22)$$

where \ddot{q}_{ji} , with $i = 1, 2$, is given by:

$$\ddot{q}_{ji} = \psi_{ji} \left(\tau_{f_{ji}} - S_{ji}^T \left(M_{ji}^A \dot{S}_{ji} \dot{q}_{ji} + W_{ji}^A \right) \right) \quad (23)$$

Afterwards, the articulated inertia M_1^A and bias wrench W_1^A for the base are computed as

$$\begin{aligned} M_1^A &= M_{B_1}^0 + M_{B_5}^0 + \sum_{j=2}^4 (M_{j1}^A - M_{j1}^A S_{j1} \psi_{j1} S_{j1}^T M_{j1}^A), \\ W_1^A &= -\text{ad}_{V_1^0}^T (M_{B_1}^0 + M_{B_5}^0) V_1^0 - W_{app, B_1}^0 - W_{grav, B_1}^0 - W_{grav, B_5}^0 \\ &\quad + \sum_{j=2}^4 (M_{j1}^A (S_{j1} \ddot{q}_{j1} + \dot{S}_{j1} \dot{q}_{j1}) + W_{j1}^A). \end{aligned} \quad (24)$$

Hence, the following six linear equations are solved for the base acceleration twist \dot{V}_1^0 using LDL^T method, since M_1^A is symmetric positive definite

$$0 = M_1^A \dot{V}_1^0 + W_1^A. \quad (25)$$

The obtained value of \dot{V}_1^0 is then used to retrieve the joint accelerations by evaluating the following expressions:

$$\begin{aligned} \ddot{q}_{j1} &= -\psi_{j1} S_{j1}^T M_{j1}^A \dot{V}_1^0 + \ddot{q}_{j1} \\ \dot{V}_{j1}^0 &= \dot{V}_1^0 + S_{j1} \ddot{q}_{j1} + \dot{S}_{j1} \dot{q}_{j1} \\ \ddot{q}_{j2} &= -\psi_{j2} S_{j2}^T M_{j2}^A \dot{V}_1^0 + \ddot{q}_{j2}. \end{aligned} \quad (26)$$

V. SIMULATION TESTS

This section presents simulation results designed to establish confidence in the generalizability of our findings beyond the standard model used for formal proofs. To achieve this, we evaluate the proposed controller using a more complex model that incorporates non-idealities such as noise and uncertain parameters. To show that the main body B_1 of the proposed MAV (4), with the state feedback controller in (17) (20) whose dynamics are given in (16), is capable of stabilizing its attitude independently from its position and vice versa in both designs PJD₁ and PJD₂, two indicative values for the base pose at equilibrium are selected. The attitude set point is chosen such that the MAV stabilizes a base configuration making the desired frame \mathcal{F}_b rotated around the inertial frame y_w -axis by 60° , i.e., $C_{1e}^0 = \begin{pmatrix} R_{1e}^0 & 0_{3 \times 1} \\ 0_{1 \times 3} & 1 \end{pmatrix}$ with $R_{1e}^0 = R_x(0)R_y(60^\circ)R_z(0)$, whereas the position step reference is formed by the desired C_{1e}^0 pose having a constant orientation and a position of \mathcal{F}_b 's origin equal to 1 m along the y_w -axis, i.e., $C_{1e}^0 = \begin{pmatrix} I_{3 \times 3} & (0 \ 1 \ 0)^T \\ 0_{1 \times 3} & 1 \end{pmatrix}$. The position reference is applied for the first 60 seconds of the simulation. Upon convergence to the desired position, the attitude maneuver starts. The corresponding state and input evolutions over time are reported in Fig. 3.

The orientation and position errors of frame \mathcal{F}_b are denoted by $e_{\phi_{1,l}}$ and $e_{p_{1,l}}$, respectively, with $l = \{x, y, z\}$. $e_{\phi_{1,l}}$ is defined as $e_{\phi_{1,l}} := \phi_{e,l} - \phi_l$ where $\phi_{e,l}$ and ϕ_l are the desired and actual angles resulting from transforming the rotation matrices in C_{1e}^0 and C_1^0 to the Euler angles sequence XYZ during the simulation time, respectively. $e_{p_{1,l}}$ is given by $e_{p_{1,l}} := p_{e,l} - p_l$ where p_e and p are the desired and actual position vectors of \mathcal{F}_b 's origin in the inertial frame, respectively. The $e_{w_1^0}$ and $e_{v_1^0}$ are the evolution of the angular and linear velocities components of the base twist V_1^0 , respectively.

To better emulate realistic conditions, the simulation in Fig. 3 includes parametric uncertainty and input noise. The noise is a low-pass filtered Gaussian noise with a state $\beta(t) \in \mathbb{R}^6$ and dynamics

$$\dot{\beta}(t) = -k\beta(t) + \mu, \quad \mu \in \mathcal{N}(0, l^2 I_{6 \times 6}), \quad (27)$$

where $l = 0.1$ and $k = 45$. Fig. 6 shows the components of the noise $\beta(t)$ added to the actuators during the simulation in Fig. 3. The true parameter values, listed in Table II, are each perturbed by $+5\%$. Additionally, the initial conditions are

Parameter	Value	Unit	Description
m_p	0.5	kg	Link B_j mass, $j = 2, 3, 4$
m_a	0.5	kg	Link B_5 mass
m_b	1.0	kg	Base B_1 mass
a	0.5	m	Length between any two adjacent joints
c	0.25	m	Length from a joint to the respective B_j 's CoM
g	9.81	m/s ²	Gravitational acceleration
I_{px}	2.1875×10^{-3}	kg·m ²	Link B_j inertia about x_p -axis
I_{py}	2.1875×10^{-3}	kg·m ²	Link B_j inertia about y_p -axis
I_{pz}	1.168×10^{-6}	kg·m ²	Link B_j inertia about z_p -axis
I_{bx}	8.3333×10^{-3}	kg·m ²	Inertia of base B_1 about x_b -axis
I_{by}	8.3333×10^{-3}	kg·m ²	Inertia of base B_1 about y_b -axis
I_{bz}	1.6667×10^{-2}	kg·m ²	Inertia of base B_1 about z_b -axis
b_{fx}	0.9	N.m.s/rad	Viscous friction coefficient about e_{j1} -axis
b_{fy}	0.9	N.m.s/rad	Viscous friction coefficient about e_{j2} -axis
$ k $	0.01	m	Ratio of drag-trust coeff. for B_j 's propeller

TABLE II: Plant Parameters with Definitions and Units

not an admissible equilibrium and given by $(q_t(0), q_5(0)) = 0.1 \times \mathbf{1}_{8 \times 1} \text{ rad}$, $x_2(0) = \mathbf{0}_{12 \times 1}$, and $f(0) = 1.05 f_e^{[2]}$, with $f_e^{[2]}$ calculated from (49). The initial base configuration for simulation in Fig. 3 is $C_1^0(0) = \begin{pmatrix} R_1^0(0) & (1 \ -1 \ -1)^T \\ 0_{1 \times 3} & 1 \end{pmatrix}$ with $R_1^0(0) = R_x(-60^\circ)R_y(-30^\circ)R_z(60^\circ)$, introducing initial attitude and position errors.

To cope with parametric uncertainty, the version of the virtual control including an integral term (108) in Remark 3 is utilized to eliminate the steady state error. The controller gains $\bar{K}_d = \text{diag}(5.5576)$ and $\bar{K}_a = \text{diag}(14.9433)$ are obtained from applying LQR on the error linear system (107), with weighting matrices on its state $Q = \text{diag}(0.0001) \in \mathbb{R}^{12 \times 12}$ and input $R = \text{diag}(0.0001) \in \mathbb{R}^{6 \times 6}$, while $K_I = \text{diag}(60)$ is selected by trial-and-error to zero the steady-state error. The gain matrix $K_p = \text{diag}(0.1)$ appearing in the kinematics controller (92) affects how fast $C_1^0(t)$ is desired to converge to C_{1e}^0 , which in turn reflects on how fast the reference trajectory $\zeta_{1e}(t)$ in the error system (107) evolves. When the closed-loop error system (107) operates with fixed values of \bar{K}_d and \bar{K}_a , the higher this K_p gain is, the larger the error state values become, requiring greater thrusts and faster tilting speed of the actively-tilting propeller.

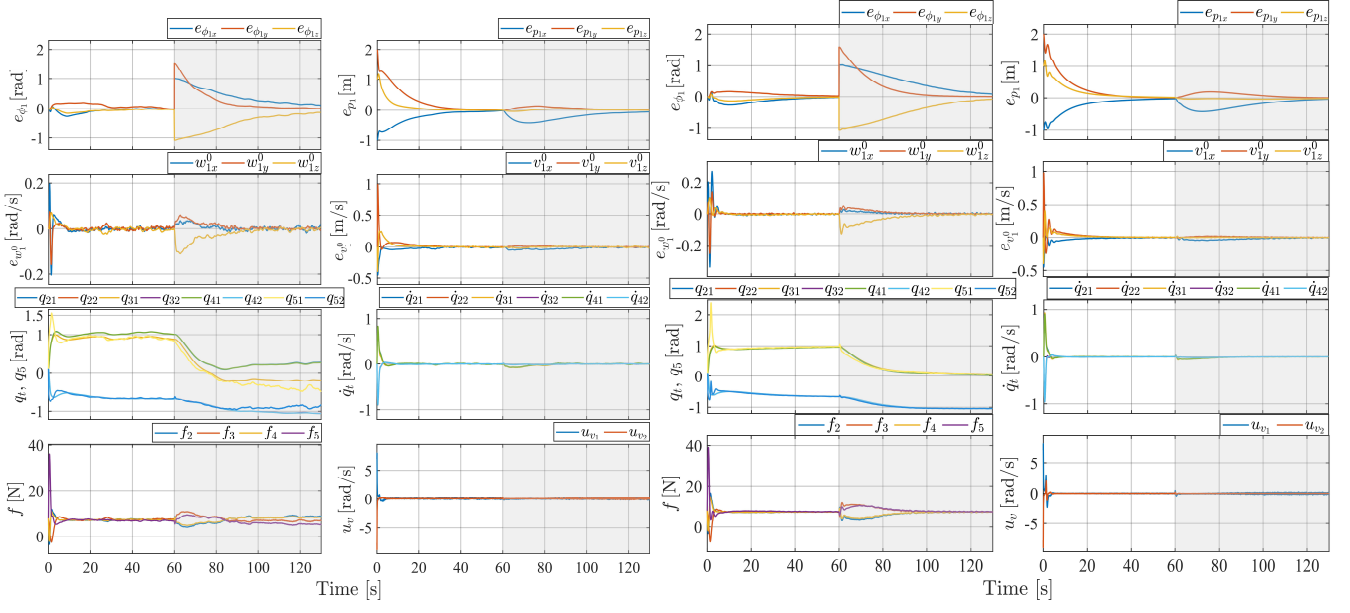
Furthermore, to show that the zero dynamics (78) in the simulations has a stable behavior as formally proven in Sec. VII-C for the standard model, we simulated its evolution for initial conditions $C_1^0(0) = I_{4 \times 4}$, $q_t(0) = -30^\circ \times \mathbf{1}_{6 \times 1}$, $\dot{q}_t(0) = 0.1 \text{ rad/s} \times \mathbf{1}_{6 \times 1}$ in the nominal settings. The results in Fig. 4 indicate convergence to zero of the passive joint variables and corresponding speeds, which is indeed the corresponding joint equilibrium in \bar{x}_e for the base pose $C_{1e}^0 = C_1^0(0) = I_{4 \times 4}$.

We conclude by highlighting the main difference between PJD₁ and PJD₂ by comparing the total thrust magnitudes for the scenario in Fig. 3. It can be observed from Fig. 5 that PJD₁ equilibrium thrust satisfies $\sum_{j=2}^5 f_{je}^{[1]} > \sum_{j=2}^5 f_{je}^{[2]}$ with $f_e^{[2]} = f_{min} \in \mathcal{F}_{min}^{\text{eq}}$. In fact, for this desired C_{1e}^0 , the residual torque is $\tau_{dj} \neq 0$ and thus the corresponding joint equilibrium $q_t^{[1]}$ yields an equilibrium thrust $f_e^{[1]}$ satisfying $\sum_{j=2}^5 f_{je}^{[1]} \approx 1.02 f_{min}$, hence witnessing about 2% increase over the minimal value $f_e^{[2]}$, which is achieved in PJD₂, reinforcing the findings in Proposition 1.

Videos for the numerical simulations in Fig. 3 are available at <https://tinyurl.com/bdur26au>.

VI. CONCLUSION

In this work, we have presented a novel MAV design idea that attains omnidirectionality in the 3D space with no internal force at the equilibrium and with minimum number of actuators. This is accomplished by first introducing the proposed vehicle's dynamical model composed of a main body (base), whose configuration evolves on $SE(3)$ thus avoiding the singularity issues stemming from using local coordinates for the configuration manifold, and 4 propeller-carrying links connected to this base by 4 universal joints, 3 of which are passive.



(a) PJD1

(b) PJD2

Fig. 3: Time evolutions of the state and input for a common simulation are presented for two designs: (a) PJD₁ and (b) PJD₂. The simulation comprises two phases. First (0-60s), a step reference of 1m along the inertial y_w axis is commanded for the base position, with the initial attitude held constant. Second (60-130s, gray-shaded), a step reference demands a 60° rotation about the inertial y_w axis for the attitude, while the position at $t = 60$ s is maintained. Imperfections such as large initial errors, uncertainty, and noise contribute to the angular velocity and attitude errors during both the initial position maneuver and the subsequent attitude maneuver

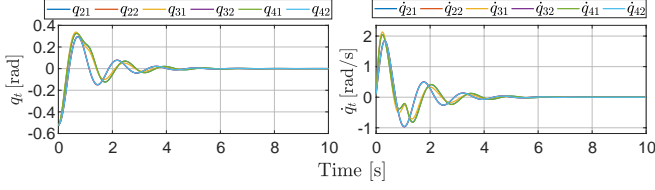


Fig. 4: Time evolution of the zero dynamics states showing convergence.

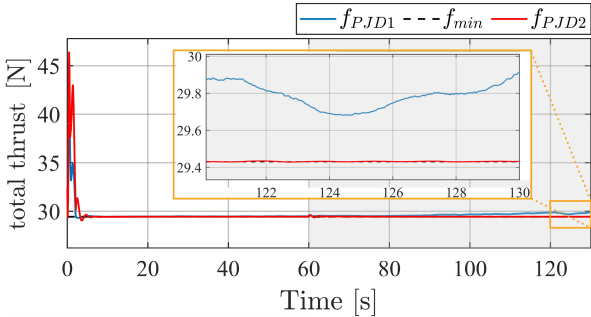


Fig. 5: Comparison of the total thrust evolution between PJD₁ and PJD₂ for the same scenario in Fig. 3. In steady state, PJD₂ thrust magnitudes sum up to exactly the minimal value (9), unlike its PJD₁ counterpart, which is about 2% higher (still much better compared to the internal forces required by state of the art designs).

Afterward, the equilibrium set is derived. This vehicle has an equilibrium for the joint positions at every pose of the base. If the universal joints are additionally equipped with a torsion spring, the sum of thrust magnitudes produced at such equilibrium becomes precisely the vehicle's weight whereas their directions are aligned vertically in the world

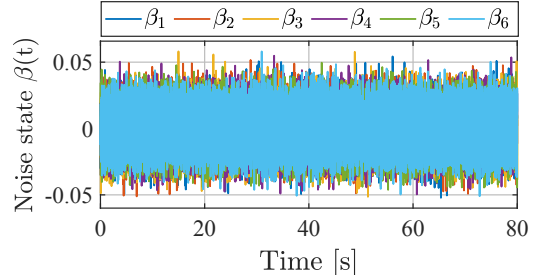


Fig. 6: Evolution of noise states added to the inputs in the simulation in Fig. 3.



Fig. 7: Possible implementation of the proposed concept in Fig. 1. The vehicle can perform a large range attitude maneuver around any axis while keeping the propellers vertical thanks to the 2-DoF joints between the base and the propellers.

frame, resulting in eliminating internal forces at any base pose in steady state. This is achieved with no overactuation, contrarily to state-of-the-art solutions. However, if no spring is added, the amount of internal forces can still be made arbitrarily small by carefully choosing the characteristics of the attached links.

By proving that the zero dynamics, represented by the

passive joints dynamics, is asymptotically stable, any base pose can be rendered asymptotically stable for the proposed MAV under a dynamic state feedback controller, as long as the extended system state trajectories remain in a certain neighborhood, which is constructed based on applying 1-step of the dynamic extension algorithm [23] followed by feedback linearization on the I/O map in a neighborhood of the desired equilibrium. The remaining virtual input is then obtained by implementing a backstepping strategy, taking the base configuration error as the left-trivialized error on $SE(3)$. Furthermore, to implement this dynamic controller efficiently, we introduced a method to evaluate the acceleration recursively without resorting to the inversion of the generalized mass matrix or numerical differentiation schemes.

While the simulation shows that the proposed MAV can perform decoupled motions even in presence of non-idealities, this might require the system trajectories to stay close to the neighborhood boundary, especially when the desired maneuver makes the actively-tilting thrust approach zero, leading to surges in the control variables. Future work will focus on developing a control scheme that overcomes this limitation in parallel with investigating the case with more generic (non-coplanar) propellers arrangements, relaxing the assumptions on the actively-tilting propeller link, and extending the control scheme to handle trajectory tracking problems. Providing experimental validation of the proposed concept will also receive attention. A possible mechanical design is displayed in Fig. 7, which supports the potential technological value of the proposed work; however, the realization of the mechatronics prototype requires considerable additional effort and represents non-negligible future work which is beyond the scope of the research presented in this paper.

ACKNOWLEDGMENTS

The authors gratefully acknowledge Quentin Sablé (University of Twente; q.l.g.sable@utwente.nl) for producing some of the figures used in this work.

VII. PROOFS

A. Proof of Lemma 1

1) *Necessity Proof:* Assume that at least one propeller, labeled l , is not vertical in the inertial frame, hence $C_l^0(\bar{C}_1^0, \alpha_l) e_3 \neq e_3$. The thrust force vector of propeller i , expressed in the inertial frame, is denoted by $T_i^0 = f_i \alpha_i$. When the MAV is at equilibrium, the resultant thrust force in the inertial frame must satisfy $T_{tot}^0 = m_{tot}g(0\ 0\ 1)^T$ to compensate for the gravitational force. Thus, this constraint must hold at equilibrium

$$\sum_{i=1}^{l-1} f_i (0\ 0\ 1)^T + f_l (\alpha_{lx} \alpha_{ly} \alpha_{lz})^T = m_{tot}g (0\ 0\ 1)^T \quad (28)$$

$$\sqrt{\alpha_{lx}^2 + \alpha_{ly}^2 + \alpha_{lz}^2} = 1 \quad (29)$$

Expanding this yields

$$f_l \alpha_{lx} = 0, \quad f_l \alpha_{ly} = 0, \quad f_l \alpha_{lz} = m_{tot}g - \sum_{i=1}^{l-1} f_i \quad (30)$$

If $f_l > 0$ then (30) gives $(\alpha_{lx}, \alpha_{ly}) = (0, 0)$. This makes (29) have only two possible solution $\alpha_{lz} = \pm 1$. Setting $\alpha_{lz} = 1$ in (30) yields $\sum_{i=1}^{l-1} f_i < m_{tot}g$. This solution for α_l is in a contradiction with the assumption as it implies that $C_l^0(\bar{C}_1^0, \alpha_l) e_3 = e_3$ is true, i.e. propeller l is vertical in the inertial frame, and (30) admits a solution of $f_i = \frac{1}{l}m_{tot}g$. As a result, $f \in \mathcal{F}_{\min}^{\text{eq}}$ and no internal force is generated at equilibrium. If instead $f_l > 0$ and $(\alpha_{lx}, \alpha_{ly}, \alpha_{lz}) = (0, 0, -1)$, then from (30) we have $\sum_{i=1}^{l-1} f_i > m_{tot}g$. While this is not a contradiction, it leads to $f \in \mathcal{F}_{\text{int.for.}}^{\text{eq}}$. Hence, the assumption $C_l^0(\bar{C}_1^0, \alpha_l) e_3 \neq e_3$ does not hold when $f \in \mathcal{F}_{\min}^{\text{eq}}$, proving the necessary condition by contradiction. By induction, the same steps can be easily repeated to cases where two or more propellers assume $C_l^0(\bar{C}_1^0, \alpha_l) e_3 \neq e_3$.

2) *Sufficiency Proof:* If all propellers point up at equilibrium, i.e. $C_i^0(\bar{C}_1^0, \alpha_i) e_3 = e_3 \forall i \in \{1, \dots, l\}$, then this renders all direction vectors α_i 's equal to $(0\ 0\ 1)^T$, which automatically satisfies (28) with $f_i = \frac{1}{l}m_{tot}g$. Hence, $f \in \mathcal{F}_{\min}^{\text{eq}}$.

B. Proof of Proposition 1

The proof is constructive and divided into two parts. In the first part, Statement 1 is proven by finding PJD_2 joint equilibrium configurations $q_{te}^{[2]}$ from (8) for any given base pose $C_{1e}^0 \in SE(3)$ and showing that the associated equilibrium thrust $f_e^{[2]}$ belongs to the minimal equilibrium thrust $\mathcal{F}_{\min}^{\text{eq}}$ defined in (9) and remains fixed for any such pose C_{1e}^0 , rendering Statement 2 an immediate corollary as the condition $f_e^{[2]} \in \mathcal{F}_{\min}^{\text{eq}}$ implies that no excess thrust is present at any C_{1e}^0 , i.e. $f_e^{[2]} \notin \mathcal{F}_{\text{int.for.}}^{\text{eq}}$. (Definition 9).

In the second part, we start by solving (7) for $q_{te}^{[1]}$. We then illustrate that, when $\tau_{dj} \neq 0$, there is no joint equilibrium satisfying $C_j^0(C_{1e}^0, q_{je}^{[1]}) e_3 = e_3$, hence by Lemma 1, no minimal thrust is produced at these equilibria $q_{je}^{[1]}$, which is the subject of statement 3. Once again, statement 4 follows as a result since $C_j^0(C_{1e}^0, q_{je}^{[1]}) e_3 \neq e_3$ necessarily implies $f_e^{[1]} \in \mathcal{F}_{\text{int.for.}}^{\text{eq}}$. However, we observe that $f_e^{[1]}$, when $\tau_{dj} \neq 0$, $f_e^{[1]}$ can be made arbitrarily close to the set $\mathcal{F}_{\min}^{\text{eq}}$ (9), i.e. $q_{te}^{[1]}$ is arbitrarily close to meet $C_j^0(C_{1e}^0, q_{je}^{[1]}) e_3 = e_3$, by changing the link parameters.

1) *Statement 1 Proof:* Expanding the LHS of (8) or (7) for any $B_j \forall j = 2, 3, 4$ yields the pair of equations for B_j

$$g_{t_j} = -S_j^T W_{grav, B_j}^0 = (-S_{j1}^T - S_{j2}^T)^T M_{B_j}^0 G^0 \quad (31)$$

where the instantaneous spatial joint screws are given by $S_{j1}(C_1^0) = \text{Ad}_{C_1^0} Y_{j1}$ and $S_{j2}(C_1^0, q_{j1}) = \text{Ad}_{C_{j1}^0} \text{Ad}_{A_{j1}^0}^{-1} Y_{j2}$, with A_{j1}^0 being the configuration of the intermediate link \bar{B}_j frame, placed at the center of rotation of q_{j1} , connecting B_1 and B_j when the vehicle is in the home configuration shown in Fig. 1, and C_{j1}^0 being its configuration in a generic vehicle pose. $Y_{ji} \in se(3)$ is the constant spatial screw of q_{ji} in home configuration. For details on screw theory, consult [25].

Now, consider the LHS of first equation in (31), which is written as

$$\begin{aligned} g_{t_{j1}} &= -S_{j1}^T M_{B_j}^0 (0_{1 \times 5} - g)^T \\ &= Y_{j1}^T \text{Ad}_{C_j^0}^T \text{Ad}_{C_j^0}^{-T} I_{B_j}^j \text{Ad}_{C_j^0}^{-1} \bar{e}_6^6 g \end{aligned} \quad (32)$$

where $I_{B_j}^j$ is the diagonal B_j 's CoM-referred inertia tensor. $\bar{e}_i^k \in \mathbb{R}^k$ is a zero vector with 1 in the i -th component. Since the adjoint matrix $\text{Ad}_{C_j^0}^{-T}$ has the properties

$$\begin{aligned} \text{Ad}_{C_j^0}^{-T} &= \text{Ad}_{C_j^0}^T = (\text{Ad}_{C_1^0} C_1^0)^T = (\text{Ad}_{C_1^0} \text{Ad}_{C_1^0})^T \\ &= \text{Ad}_{C_1^0}^T \text{Ad}_{C_1^0}^{-T} = \text{Ad}_{C_1^0}^{-T} \text{Ad}_{C_1^0}^{-T} \end{aligned} \quad (33)$$

substituting $\text{Ad}_{C_j^0}^{-T} = \text{Ad}_{C_1^0}^{-T} \text{Ad}_{C_1^0}^{-T}$ in (32) gives

$$g_{t_{j1}} = Y_{j1}^T \text{Ad}_{C_j^0}^{-T} I_{B_j}^j \text{Ad}_{C_j^0}^{-1} \bar{e}_6^6 g = Y_{j1}^T \text{Ad}_{C_1^0}^{-T} I_{B_j}^j \bar{r}_j g \quad (34)$$

where \bar{r}_j denotes

$$\bar{r}_j = \text{Ad}_{C_j^0}^{-1} \bar{e}_6^6 \quad (35)$$

Observe that substituting $\bar{r}_j = \bar{e}_6^6$ in (34) reduces it to

$$\begin{aligned} g_{t_{j1}} &= Y_{j1}^T \text{Ad}_{C_1^0}^{-T} I_{B_j}^j \bar{e}_6^6 g \\ &= Y_{j1}^T \text{Ad}_{C_1^0}^{-T} \bar{e}_6^6 m_p g \end{aligned} \quad (36)$$

where $g_{t_{j1}}$ now depends only on q_j . Since the constant screw is $Y_{j1}^T = ((\bar{e}_1^3)^T \sigma_j \frac{a}{2} (\bar{e}_3^3)^T)$, where $\sigma_j = 1$ for $j = 2, 5$ and $\sigma_j = -1$ otherwise, (36) can be manipulated further as

$$\begin{aligned} g_{t_{j1}} &= ((\bar{e}_1^3)^T \sigma_j \frac{a}{2} (\bar{e}_3^3)^T) \begin{pmatrix} R_j^1 & -[P_j^1]^T R_j^1 \\ 0_{3 \times 3} & R_j^1 \end{pmatrix} \bar{e}_6^6 m_p g \\ &= ((\bar{e}_1^3)^T \sigma_j \frac{a}{2} (\bar{e}_3^3)^T) \begin{pmatrix} -[P_j^1]^T R_j^1 \bar{e}_3^3 \\ R_j^1 \bar{e}_3^3 \end{pmatrix} m_p g \\ &= (\sigma_j \frac{a}{2} (\bar{e}_3^3)^T - (\bar{e}_1^3)^T [P_j^1]^T) R_j^1 \bar{e}_3^3 m_p g \\ &= 0 \equiv \text{RHS of first equation in (8)}. \end{aligned} \quad (37)$$

where $C_j^1 = \begin{pmatrix} R_j^1 & P_j^1 \\ 0_{1 \times 3} & 1 \end{pmatrix}$. Hence setting $\bar{r}_j = \bar{e}_6^6$ satisfies the first equation in (8).

Next, let us consider the second equation in (8). Simplifying using the properties in (33), and substituting the expression of the constant screw Y_{j2} , configuration A_{j1}^0 and \bar{r}_j (35) yield

$$\begin{aligned} g_{t_{j2}} &= Y_{j2}^T \text{Ad}_{A_{j1}^0}^{-T} \text{Ad}_{C_{j1}^0}^T \text{Ad}_{C_{j1}^0}^{-T} I_{B_j}^j \text{Ad}_{C_{j1}^0}^{-1} \bar{e}_6^6 g \\ &= Y_{j2}^T \text{Ad}_{A_{j1}^0}^{-T} \text{Ad}_{C_{j1}^0}^{-T} I_{B_j}^j \bar{r}_j g \\ &= ((\bar{e}_2^3)^T 0_{1 \times 3}) \text{Ad}_{C_{j1}^0}^{-T} I_{B_j}^j \bar{r}_j g \end{aligned} \quad (38)$$

Setting $\bar{r}_j = \bar{e}_6^6$ gives

$$\begin{aligned} g_{t_{j2}} &= ((\bar{e}_2^3)^T 0_{1 \times 3}) \text{Ad}_{C_{j1}^0}^{-T} \bar{e}_6^6 m_p g \\ &= ((\bar{e}_2^3)^T 0_{1 \times 3}) \begin{pmatrix} -[P_j^{j1}]^T R_j^{j1} \bar{e}_3^3 \\ R_j^{j1} \bar{e}_3^3 \end{pmatrix} m_p g \\ &= -(\bar{e}_2^3)^T [P_j^{j1}]^T R_j^{j1} \bar{e}_3^3 m_p g \\ &= (-\cos(q_{j2e}) 0 \sin(q_{j2e})) \begin{pmatrix} \sin(q_{j2e}) \\ 0 \\ \cos(q_{j2e}) \end{pmatrix} c m_p g \\ &= 0 \equiv \text{RHS of second equation in (8)}. \end{aligned} \quad (39)$$

We conclude that $\bar{r}_j = \bar{e}_6^6$ satisfies (8). Observe that this condition implies that all propellers are aligned vertically in the inertial frame at equilibria for any $C_{1e}^0 \in SE(3)$. To see this, expand (35) as

$$\bar{r}_j = \bar{e}_6^6 = \text{Ad}_{C_j^0}^{-1} \bar{e}_6^6 \quad (40)$$

$$\begin{pmatrix} 0_{3 \times 1} \\ \bar{e}_3^3 \end{pmatrix} = \begin{pmatrix} R_0^j & 0_{3 \times 3} \\ -R_0^j [P_j^0] & R_0^j \end{pmatrix} \begin{pmatrix} 0_{3 \times 1} \\ \bar{e}_3^3 \end{pmatrix} = \begin{pmatrix} 0_{3 \times 1} \\ R_0^j \bar{e}_3^3 \end{pmatrix}$$

Hence $\bar{e}_3^3 = R_0^j (R_{1e}^0, q_{je}^{[2]}) \bar{e}_3^3 \forall j = 2, 3, 4, 5$, or alternatively $C_j^0 e_3 = e_3$ using Lemma 1 notation. This also gives the expression of $q_{je}^{[2]}$ by solving $\bar{r}_j = \bar{e}_6^6$ for $q_{je}^{[2]}$ as

$$R_0^1 e_3 = R_j^1 (q_{je}^{[2]}) \bar{e}_3^3 = R_x (q_{j1e}^{[2]}) R_y (q_{j2e}^{[2]}) \bar{e}_3^3 \quad (41)$$

Thus we have the solution $q_{je}^{[2]}$ as

$$\begin{aligned} l_{s1} &= \frac{-r_{32}}{\sqrt{1 - r_{31}^2}}, l_{c1} = \sqrt{1 - l_{s1}^2} \\ l_{s2} &= r_{31}, l_{c2} = \sqrt{1 - l_{s2}^2} \\ q_{j1e}^{[2]} &= \text{atan}(l_{s1}, l_{c1}) \forall i = 1, 2, j = 2, 3, 4, 5 \end{aligned} \quad (42)$$

where r_{mn} is the element (m, n) in any desired base orientation at PJD_2 equilibrium R_{1e}^0 . Notice that $q_{je}^{[2]}$ is equal for any attached link B_j . Moreover, it is always possible to obtain this solution $q_{je}^{[2]}$ (42) for every $R_1^0 \in SO(3)$ since aligning the unit vector $R_j^1 (q_{je}^{[2]}) \bar{e}_3^3 =: z_j^1$, where $z_j^1 \in \mathbb{S}^2$ is the z-axis of \mathcal{F}_{p_j} expressed in \mathcal{F}_b , with any desired unit vector $z_0^1 \in \mathbb{S}^2$ in \mathcal{F}_b , where $R_0^1 \bar{e}_3^3 =: z_0^1$, requires only 2 variables, i.e. $q_{j1e}^{[2]}, q_{j2e}^{[2]}$, as $\dim(\mathbb{S}^2) = 2$ when the manifold \mathbb{S}^2 is embedded in the 3-dimensional Euclidean vector space.

Now, we show that the associated thrust $f_e^{[2]} \in \mathcal{F}_{\min}^{\text{eq}}$ and fixed for any C_{1e}^0 . The dynamics of base at any static equilibrium reduces to

$$g_b(C_{1e}^0, q_{te}) = -W_{app,b}^0(f_e, q_{te}, q_{5e}) \quad (43)$$

which reads explicitly as

$$\sum_{j=2}^5 \text{Ad}_{(C_{f_j}^0)^{-1}}^T \bar{f}_j f_{je} = \sum_{j=1}^5 \text{Ad}_{(C_j^0)^{-1}}^{-T} I_{B_j}^j \text{Ad}_{(C_j^0)^{-1}}^{-1} \bar{e}_6^6 g \quad (44)$$

Substituting $\bar{r}_j = (0_{3 \times 1} \bar{r}_j)$ from (35) yields

$$\begin{aligned} \sum_{j=2}^5 \left((I k_j - [P_j^1]^T) R_j^1 \bar{e}_3^3 \right) f_{je} &= g m_b \begin{pmatrix} 0_{3 \times 1} \\ R_0^1 \bar{e}_3^3 \end{pmatrix} \\ &+ g \sum_{j=2}^5 m_j \begin{pmatrix} -[P_j^1]^T R_j^1 \hat{r}_j \\ R_j^1 \hat{r}_j \end{pmatrix} \end{aligned} \quad (45)$$

where I is the identity matrix. Using the property $R_j^1 [R_1^j P_j^1] = -[P_j^1]^T R_j^1$ and $R_j^1 \hat{r}_j = R_0^1 \bar{e}_3^3$, we get

$$\begin{aligned} \sum_{j=2}^5 R_j^1 (I k_j + [R_1^j P_j^1]) \bar{e}_3^3 f_{je} &= g \left(\sum_{j=2}^5 R_j^1 [R_1^j P_j^1] \hat{r}_j m_j \right) \\ \sum_{j=2}^5 R_j^1 \bar{e}_3^3 f_{je} &= g \sum_{j=2}^5 R_j^1 \hat{r}_j \left(\frac{1}{4} m_b + m_j \right) \end{aligned} \quad (46)$$

Since in PJD₂, $q_{je}^{[2]} \forall j = 2, 3, 4, 5$ are equal, R_j^1 can be taken as a common factor, hence pre-multiplying by R_1^j gives

$$\begin{aligned} \sum_{j=2}^5 k_j f_{je}^{[2]} \bar{e}_3^3 + \sum_{j=2}^5 [R_1^j P_j^1] f_{je}^{[2]} \bar{e}_3^3 &= g \left(\sum_{j=2}^5 [R_1^j P_j^1] m_j \right) \bar{e}_3^3 \\ \bar{e}_3^3 \sum_{j=2}^5 f_{je}^{[2]} &= \bar{e}_3^3 \sum_{j=2}^5 g \left(\frac{1}{4} m_b + m_j \right) \end{aligned} \quad (47)$$

After $\hat{r}_j = \bar{e}_3^3$ is substituted. The second equation is satisfied with $f_{je}^{[2]} = g(\frac{1}{4} m_b + m_j)$, hence $f_e^{[2]} \in \mathcal{F}_{\min}^{\text{eq}}$. Substituting this $f_{je}^{[2]}$ make the first equation reduce to

$$\sum_{j=2}^5 k_j g \left(\frac{1}{4} m_b + m_j \right) \bar{e}_3^3 + \sum_{j=2}^5 [R_1^j P_j^1] \bar{e}_3^3 = 0 \quad (48)$$

thus $\sum_{j=2}^5 k_j g \left(\frac{1}{4} m_b + m_j \right) = 0$ since $\sum_{j=2}^5 [R_1^j P_j^1] \bar{e}_3^3 = 0$ is always true at any $q_{je}^{[2]}$ (42). We conclude that the associated thrust at $q_{je}^{[2]}$ is, when $m_j = m_p \forall j = 2, 3, 4, 5$

$$f_{je}^{[2]} = g \left(\frac{1}{4} m_b + m_p \right), \text{ with } k_i \text{ chosen by } \sum_{j=2}^5 k_i = 0 \quad (49)$$

2) *Statement 2 Proof:* Since $f_e^{[2]} \in \mathcal{F}_{\min}^{\text{eq}}$ is proven in Statement 1, it follows from Definition 1 that no internal forces are generated $f_e^{[2]} \notin \mathcal{F}_{\text{int.for.}}$ at the corresponding equilibrium configurations associated with this $f_e^{[2]}$, i.e. $q_{te}^{[2]}$ in (42) and any desired $C_{1e}^0 \in SE(3)$.

3) *Statement 3 Proof:* In Sec. VII-B.1, it is found that when all propellers point up in the inertial frame, i.e. $\bar{r}_j = \bar{e}_6^6$ or $C_{1e}^0 e_3 = e_3 \forall j = 2, 3, 4, 5$, the LHS of (7) becomes $g_{tj}(C_{1e}^0, q_{te}) = 0$. Since the RHS of of it for any j is equal to (τ_{dj}^0) , which is not zero when $\tau_{dj} \neq 0$, $C_j^0(C_{1e}^0, q_{je}^{[1]}) e_3 \neq e_3$ must hold true. Thus, from Lemma 1, no minimal thrust is produced at any PJD₁ equilibrium $f_e^{[1]} \notin \mathcal{F}_{\min}^{\text{eq}} \forall \tau_{dj} \neq 0$.

For completeness, we proceed to find conditions on $q_{je}^{[1]}$, similar to $\bar{r}_j = \bar{e}_6^6$ obtained for PJD₂, that must be met at any base equilibrium C_{1e}^0 . We start from (38) and substitute the values of the constant screws, constant transformations and $\bar{r}_j = (0_{3 \times 1} \hat{r}_j)$, which yields

$$-(\bar{e}_2^3)^T [P_j^{j1}]^T R_j^{j1} \hat{r}_j m_j g = 0 \quad (50)$$

which is satisfied when $\hat{r}_j = (0 \hat{r}_{j,1} \hat{r}_{j,2})$, $\hat{r}_{j,2} = \sqrt{1 - \hat{r}_{j,1}^2}$. in PJD₁, (34) has the RHS equal to $S_{j1}^T W_{app,B_j}^0$. This can be expressed as

$$\begin{aligned} (\sigma_j \frac{a}{2} (\bar{e}_3^3)^T - (\bar{e}_1^3)^T [P_j^1]^T) R_j^1 (\hat{r}_j m_j g - \bar{e}_3^3 f_{je}^{[1]}) \\ + (\bar{e}_1^3)^T R_j^1 \bar{e}_3^3 k_j f_{je}^{[1]} = 0 \end{aligned} \quad (51)$$

since

$$Y_{j1}^T \text{Ad}_{C_j^1}^{-T} = (\cos(q_{j2e}) 0 \sin(q_{j2e}) 0 \cos(q_{j2e}) 0) \quad (52)$$

hence $q_{j2e}^{[1]}$ is constraint by

$$\cos(q_{j2e}^{[1]}) = \pm \sqrt{\frac{k_j^2 (f_{je}^{[1]})^2}{c^2 m_j^2 g^2 \hat{r}_{j,1}^2 + k_j^2 (f_{je}^{[1]})^2}} \quad (53)$$

Lastly, from (46), we have these conditions on $R_j^1(q_{je}^{[1]})$, $f_{je}^{[1]}$

$$\begin{aligned} \sum_{j=2}^5 R_j^1 k_j \bar{e}_3^3 f_{je}^{[1]} &= 0, \quad R_j^1 \hat{r}_j = R_0^1 \bar{e}_3^3 \\ \sum_{j=2}^5 [P_j^1] (R_j^1 \bar{e}_3^3 f_{je}^{[1]} - R_j^1 \hat{r}_j g m_j) &= 0 \\ \sum_{j=2}^5 R_j^1 \bar{e}_3^3 f_{je}^{[1]} - \sum_{j=2}^5 R_j^1 \hat{r}_j g \left(\frac{1}{4} m_b + m_j \right) &= 0 \end{aligned} \quad (54)$$

4) *Statement 4 Proof:* By definition 1, and Statement 3, $f_e^{[1]} \in \mathcal{F}_{\text{int.for.}}^{\text{eq}}$ immediately follows as a corollary. The amount of internal force can be made arbitrarily small if solutions of (8) and (7) are made arbitrarily close, which is realized by making the term $\frac{k_j}{cm_j} = 0$, i.e. reducing the drag-to-thrust coefficient or increasing the pendulum length or mass.

C. Proof of Theorem 1

The proof relies on the relative degree notion for MIMO affine nonlinear systems [26] and the dynamic extension algorithm for invertible systems [23] to prove Statement 1. Afterwards, we show that Statement 2 is true by a standard Lyapunov argument applied to the zero dynamics in the normal form.

1) *Statement 1 Proof:* To compute the relative degree of Σ_2 w.r.t. x_{21} , we take time derivatives of the output x_{21}

$$\dot{h}_y = \dot{V}_1^0 \quad (55)$$

From (3) \dot{V}_1^0 is expressed as

$$M_{bb} \dot{V}_1^0 = -M_{bt} \ddot{q}_t - h_b - g_b + W_{app,b}^0 \quad (56)$$

Following the approach of [27] we can express \ddot{q}_t in terms of \dot{V}_1^0 , $W_{app,t}^0$ and τ_f , hence

$$\ddot{q}_t = C_{t1} - M_{tt}^{-1} M_{bt}^T \dot{V}_1^0 + M_{tt}^{-1} W_{app,t}^0 \quad (57)$$

where C_{t1} is defined as

$$C_{t1} := M_{tt}^{-1} (\tau_f - h_t - g_t) \quad (58)$$

Substituting in (56) gives

$$\begin{aligned} (M_{bb} - M_{bt} M_{tt}^{-1} M_{bt}^T) \dot{V}_1^0 &= -M_{bt} C_{t1} - h_b - g_b \\ &\quad + W_{app,b}^0 - M_{bt} M_{tt}^{-1} W_{app,t}^0 \end{aligned} \quad (59)$$

which can be rewritten as

$$\dot{h}_y = \dot{V}_1^0 = F_1 + M_b^{-1} D_1 u \quad (60)$$

where M_b , D_1 and F_1 are defined as, with $j = 2, 3, 4$

$$\begin{aligned} M_b &= (M_{bb} - M_{bt} M_{tt}^{-1} M_{bt}^T) \\ B_j &= (I_6 - M_{B_j}^0 S_j (S_j^T M_{B_j}^0 S_j)^{-1} S_j^T) \\ \bar{D}_1 &= \left(\begin{array}{cccc} B_2 \text{Ad}_{(C_{f_2}^0)^{-1}}^T \bar{f}_2 & \cdots & \text{Ad}_{(C_{f_5}^0)^{-1}}^T \bar{f}_5 \end{array} \right) \\ D_1 &= (\bar{D}_1 \ 0_{6 \times 2}) \\ F_1 &= M_b^{-1} (-M_{bt} C_{t1} - h_b - g_b) \end{aligned} \quad (61)$$

Note that $(S_j^T M_{B_j}^0 S_j) \in R^{2 \times 2}$ is a symmetric positive definite matrix.

Since the decoupling matrix $M_b^{-1} D_1$ is singular due to D_1 being singular of rank 4 $\forall x_e \in \mathbb{D}_{x_e}^{[i]}$, system (15) does not have a vector relative degree in any open neighbourhood of the equilibrium $x_e \in \mathbb{D}_{x_e}^{[i]}$. Thus, the system is not I/O feedback linearizable by any static state feedback as the relative degree is invariant under this kind of feedback [26].

However, extending the system dynamics Σ_2 with an input precompensator, by applying the version of the dynamic extension algorithm presented in [23] for invertible nonlinear systems, may result in a system for which the vector relative degree is well-defined. Assume the precompensator takes this pure integrator form (16). Let $\bar{x} := (x_{12}, x_2, q_5, z)^T \in \bar{\mathbb{X}}$ be the extended state and $w := (\bar{w}, u_{v_1}, u_{v_2})^T$ the new input. The extended system Σ_2 can be written as $\Sigma_2 : \dot{\bar{x}} = \bar{F} + \bar{G}w$ with $\bar{F} := F + G\bar{u}$, where $\bar{u} = (z, 0, 0)^T$ and \bar{G} is given by

$$\bar{G} = \begin{pmatrix} 0_{18 \times 6} \\ 0_{2 \times 4} \quad I_{2 \times 2} \\ I_{4 \times 4} \quad 0_{2 \times 2} \end{pmatrix} \quad (62)$$

Now, we can proceed with computing the vector relative degree of Σ_2 w.r.t x_{21} by differentiating \dot{h}_y w.r.t time

$$M_{bb}\ddot{V}_1^0 = -\dot{M}_{bt}\ddot{q}_t - M_{bt}\ddot{q}_t + \dot{W}_{app,b}^0 - \dot{M}_{bb}\dot{V}_1^0 - \dot{h}_b - \dot{g}_b$$

by substituting this expression for \ddot{q}_t

$$\ddot{q}_t = C_{t2} - M_{tt}^{-1}M_{bt}^T\ddot{V}_1^0 + M_{tt}^{-1}\dot{W}_{app,t}^0 \quad (63)$$

where C_{t2} is defined as

$$C_{t2} := M_{tt}^{-1}((\dot{\tau}_f - \dot{h}_t - \dot{g}_t) - (\dot{M}_{bt}^T\dot{V}_1^0 + \dot{M}_{tt}\dot{q}_t)) \quad (64)$$

and after some algebraic manipulation it yields

$$\begin{aligned} M_b\ddot{V}_1^0 &= -\dot{M}_{bt}(C_{t1} + M_{tt}^{-1}W_{app,t}^0) - M_{bt}C_{t2} \\ &\quad + (\dot{M}_{bt}M_{tt}^{-1}M_{bt}^T - \dot{M}_{bb})\dot{V}_1^0 - \dot{h}_b - \dot{g}_b \\ &\quad - M_{bt}M_{tt}^{-1}\dot{W}_{app,t}^0 + \dot{W}_{app,b}^0 \end{aligned} \quad (65)$$

where the $\dot{h}_b, \dot{g}_b, \dot{h}_t, \dot{g}_t, \ddot{M}, \ddot{S}_j, \dot{W}^0$ are given by, $j = 2, 3, 4$

$$\begin{aligned} \dot{h}_b &= \sum_{j=2}^4 ((M_{B_j}^0 \ddot{S}_j + \ddot{M}_{B_j}^0 S_j + 2\dot{M}_{B_j}^0 \dot{S}_j) \dot{q}_j \\ &\quad + (M_{B_j}^0 \dot{S}_j + \dot{M}_{B_j}^0 S_j) \ddot{q}_j) + \dot{M}_{bb}V_1^0 + \dot{M}_{bb}\dot{V}_1^0 \\ \dot{h}_t &= \text{col}(\dot{S}_t^T((M_{B_j}^0 \dot{S}_j + \dot{M}_{B_j}^0 S_j) \dot{q}_j + \dot{M}_{B_j}^0 V_1^0) \\ &\quad + S_j^T((M_{B_j}^0 \ddot{S}_j + \ddot{M}_{B_j}^0 S_j + 2\dot{M}_{B_j}^0 \dot{S}_j) \dot{q}_j \\ &\quad + (M_{B_j}^0 \dot{S}_j + \dot{M}_{B_j}^0 S_j) \ddot{q}_j + \dot{M}_{B_j}^0 V_1^0 + \dot{M}_{B_j}^0 \dot{V}_1^0)) \\ \dot{g}_b &= -(\dot{M}_{bb} + \dot{M}_{B_5}^0)G^0 \\ \dot{g}_t &= -\dot{S}_t^T \text{col}(M_{B_j}^0 G^0) - S_t^T \text{col}(\dot{M}_{B_j}^0 G^0) \\ \ddot{M}_k^0 &= M_k^0 \text{ad}_{V_k^0}^2 + (\text{ad}_{V_k^0})^T M_k^0 + 2 \text{ad}_{V_k^0}^T M_k^0 \text{ad}_{V_k^0} \\ &\quad - M_k^0 \text{ad}_{V_k^0}^2 - \text{ad}_{V_k^0}^T M_k^0, \text{ if } k = 5 \text{ then } V_k^0 = V_1^0, \dot{V}_k^0 = \dot{V}_1^0 \\ \ddot{S}_k &= (\text{ad}_{V_k^0} + \text{ad}_{V_k^0}^2)S_k, k = 2, 3, 4 \\ \dot{W}_k^0 &= -\text{ad}_{V_k^0}^T W_k^0 + \text{Ad}_{(C_{f_5}^0)^{-1}}^T \dot{W}_k^b, k = 2, 3, 4, 5 \end{aligned} \quad (66)$$

Note that $M_{B_5}^0$ depends only on C_1^0 , i.e. $M_{B_5}^0(C_1^0)$, due to the assumptions on link B_5 . Hence, the input \dot{q}_5 does not

appear in $\dot{M}_{B_5}^0(C_1^0)$. Observe that (65) can be put in the form,

$$\ddot{h}_y = \ddot{V}_1^0 = F_2 + M_b^{-1}D_2w \quad (67)$$

where F_2 and D_2 are calculated from, with $j = 2, 3, 4$

$$\begin{aligned} D_2 &= \begin{pmatrix} B_j \text{Ad}_{(C_{f_j}^0)^{-1}}^T \bar{f}_j & \cdots & \text{Ad}_{(C_{f_5}^0)^{-1}}^T \bar{f}_5 & \bar{D}_2 \end{pmatrix} \\ \bar{D}_2 &= \begin{pmatrix} -\text{ad}_{S_{51}}^T \text{Ad}_{(C_{f_5}^0)^{-1}}^T \bar{f}_5 z_5 & -\text{ad}_{S_{52}}^T \text{Ad}_{(C_{f_5}^0)^{-1}}^T \bar{f}_5 z_5 \end{pmatrix} \\ F_2 &= M_b^{-1}(-\dot{M}_{bt}(C_{t1} + M_{tt}^{-1}W_{app,t}^0) - M_{bt}C_{t2} \\ &\quad + (\dot{M}_{bt}M_{tt}^{-1}M_{bt}^T - \dot{M}_{bb})\dot{V}_1^0 - \dot{h}_b - \dot{g}_b + \bar{W}) \\ \bar{W} &= -\sum_{j=2}^4 B_j \text{ad}_{V_j^0}^T W_{app,B_j}^0 - \text{ad}_{V_1^0}^T W_{app,B_5}^0 \end{aligned} \quad (68)$$

where C_{t1} , C_{t2} , M_b and B_j are given in (58), (64) and (61).

Because of the decoupling matrix $M_b^{-1}D_2$ of the extended system Σ_2 being full rank equal to 6 in the open neighbourhood $\mathbb{U}_{\bar{x}_e} \subseteq \bar{\mathbb{X}}$ of equilibrium $\bar{x}_e \in \mathbb{D}_{x_e}^{[i]} \cup \mathbb{D}_{f_e}^{[i]}$, system Σ_2 has a vector relative degree $(2, 2, 2, 2, 2, 2)$. Hence it can be transformed to a normal form Σ_2^H where the input/output map is linear by the means of the regular static state feedback w in (17) and the local diffomorphism $H(\bar{x}) : \mathbb{U}_{\bar{x}_e} \rightarrow \mathbb{U}_{\bar{x}_e}$

$$\begin{pmatrix} \zeta_1 \\ \zeta_2 \\ \eta \end{pmatrix} = H(\bar{x}) := \begin{pmatrix} h_y(x) \\ h_y(\bar{x}) \\ \Phi(\bar{x}) \end{pmatrix} \quad (69)$$

where $\Phi(\bar{x}) : \mathbb{U}_{\bar{x}_e} \rightarrow \mathbb{T}^6 \times \mathbb{R}^6$ is a sufficiently smooth function chosen such that, in the open neighbourhood $\mathbb{U}_{\bar{x}_e}$, $H(\bar{x})$ is a diffomorphism and $\frac{\partial \Phi}{\partial \bar{x}} G = 0$ holds. A possible choice of Φ is the states of the passive joints, as suggested in [27], $\Phi := (q_t, \dot{q}_t)^T$.

Hence the internal dynamics can be expressed as

$$\begin{aligned} \dot{\eta}_1 &= \eta_2 \\ \dot{\eta}_2 &= f_\eta(\eta_1, \eta_2, \zeta_1, \zeta_2, \bar{z}, C_1^0) \\ &:= C_{t1} - M_{tt}^{-1}M_{bt}^T\zeta_2 + M_{tt}^{-1}D_3\bar{z} \end{aligned} \quad (70)$$

where η -dynamics represent the internal dynamics and D_3 , \bar{z} are calculated from

$$\begin{aligned} \bar{z} &= (z_2 \quad z_3 \quad z_4)^T \\ D_3 &= \text{blkdiag}((k_2 s_{22}, 0)^T, (k_3 s_{32}, 0)^T, (k_4 s_{42}, 0)^T) \end{aligned} \quad (71)$$

Furthermore, we can map the controller states to the new coordinates $(z, q_5)^T = f_c(\zeta, \eta, C_1^0)$ where f_c is a solution of the algebraic equations

$$E = \tilde{D}\bar{z} + Cz_5 \quad (72)$$

where \tilde{D}, E, C are given by

$$\begin{aligned} \tilde{D} &= \text{Ad}_{C_1^0}^T \begin{pmatrix} B_2 \text{Ad}_{(C_{f_2}^0)^{-1}}^T \bar{f}_2 & B_3 \text{Ad}_{(C_{f_3}^0)^{-1}}^T \bar{f}_3 & B_4 \text{Ad}_{(C_{f_4}^0)^{-1}}^T \bar{f}_4 \end{pmatrix} \\ E &= \text{Ad}_{C_1^0}^T M_b(\zeta_2 - F_1) \\ C &= \begin{pmatrix} k_5 s_{52} - \frac{a c_{51} c_{52}}{2} \\ \frac{c_{52} (a c_{51} - 2 k_5 s_{51})}{2} \\ \frac{a (s_{52} + c_{52} s_{51})}{2} + k_5 c_{51} c_{52} \\ s_{52} \\ -c_{52} s_{51} \\ c_{51} c_{52} \end{pmatrix} \end{aligned} \quad (73)$$

Let $\bar{z} = \bar{f}_c$ where \bar{f}_c is the first 3 elements in the map f_c . Hence, substituting back into η -dynamics in (70) yields the normal form $\Sigma_2^H(\zeta, \eta; C_1^0, v)$

$$\Sigma_2^H : \begin{cases} \dot{\zeta}_1 = \zeta_2 \\ \dot{\zeta}_2 = v \\ \dot{\eta}_1 = \eta_2 \\ \dot{\eta}_2 = f_\eta(\eta_1, \eta_2, \zeta_1, \zeta_2, C_1^0, \bar{f}_c(\zeta, \eta, C_1^0)) \\ \quad := C_{t1} - M_{tt}^{-1} M_{bt}^T \zeta_2 + M_{tt}^{-1} D_3 \bar{f}_c(\zeta, \eta, C_1^0) \\ h_y = \zeta_1 \end{cases} \quad (74)$$

This proves Statement 1.

2) *Statement 2 Proof:* Σ_3 in the new coordinates becomes $\Sigma_3^H(C_1^0; \zeta_1)$

$$\dot{C}_1^0 = [\zeta_1] C_1^0 \quad (75)$$

Thus, Σ_2^H (74) interconnected with Σ_3 (75) is equivalent to the system (4) with a linear relationship between virtual input v and output from the base spatial twist V_1^0 .

The zero dynamics of the network (Σ_2^H, Σ_3^H) are the internal dynamics when $h_y(t) \equiv 0 \forall t \geq 0$. This constraint is imposed for all times by setting the virtual input $v(t) = 0 \forall t \geq 0$ and the initial conditions of ζ -dynamics to be $(\zeta_1(0), \zeta_2(0)) = (0, 0)$. As a result, the linear differential equations of ζ admit the solution $(\zeta_1(t), \zeta_2(t)) = (0, 0) \forall t \geq 0$. This also leads to Σ_3^H (75) having a solution $C_1^0(t) = C_1^0(0) \forall t \geq 0$. Thus, the zero dynamics manifold \mathbb{Z} is then obtained as

$$\mathbb{Z} = \left\{ \eta(t) \in \mathbb{T}^6 \times \mathbb{R}^6, t \in \mathbb{R}_{\geq 0} \mid \dot{\eta}(t) = \left(\begin{array}{c} \eta_2(t) \\ f_\eta(\eta_1(t), \eta_2(t), 0, 0, C_1^0(0), \bar{f}_c(0, \eta(t), C_1^0(0))) \end{array} \right) \right\} \quad (76)$$

Remark 2. In the original coordinates of system (Σ_2, Σ_3) , one can obtain the zero dynamics manifold by transforming back the the initial conditions and the input constraint $v = 0$ from the normal into the \bar{x} coordinates. Hence, $\zeta_1(0) = x_{21}(0) = 0$ while the constraint $\zeta_2(0) = \dot{x}_{21}(0) = 0$ restricts the initial conditions of the dynamic extension states $(z(0), q_5(0))^T$ to be a solution of (60) with $\dot{V}_1^0(0) = 0$. Let us call this solution f_{c_x} , then the zero dynamics manifold in the original coordinates \mathbb{Z}_x is defined by

$$\mathbb{Z}_x = \left\{ \bar{x}(t) \in \bar{\mathbb{X}}, t \in \mathbb{R}_{\geq 0} \mid \Sigma_2(\bar{x}; \tilde{w}, x_{11}(0)), \tilde{w} = -D_2^{-1} M_b F_2, x_{11}(0) \in SE(3), x_{21}(0) = 0, (z(0), q_5(0))^T = f_{c_x} \right\} \quad (77)$$

What is remaining to complete the proof is to study the stability of the zero dynamics. When $\eta \in \mathbb{Z}$ we get,

$$\begin{aligned} \dot{\eta}_1 &= \eta_2 \\ \dot{\eta}_2 &= \tilde{M}_{tt}^{-1} \left(-D_f \eta_1 - \text{col}(\tilde{S}_j^T (\tilde{M}_{B_j}^0 \dot{\tilde{S}}_j + \dot{\tilde{M}}_{B_j}^0 \tilde{S}_j) \eta_2) \right. \\ &\quad \left. + \tilde{S}_t^T \text{col}(\tilde{M}_{B_j} G^0) + D_3 \tilde{z} \right) \\ &= \tilde{M}_{tt}(\eta_1)^{-1} \left(-D_f \eta_2 - \tilde{C}(\eta_1, \eta_2) \eta_2 - \tilde{g}_t(\eta_1) + D_3(\eta_1) \tilde{z} \right) \end{aligned} \quad (78)$$

The superscript $(\tilde{\cdot})$ denotes the value of the corresponding variable evaluated at $(C_1^0(t), \zeta_1(t), \zeta_2(t)) = (C_1^0(0), 0, 0)$. \tilde{C} is the Coriolis matrix which is linear in passive joint velocities η_2 and given by

$$\begin{aligned} \tilde{C} &= \text{blockdiag}(\tilde{C}_2(\eta_{12}, \eta_{22}), \tilde{C}_3(\eta_{13}, \eta_{23}), \tilde{C}_4(\eta_{14}, \eta_{24})) \\ \tilde{C}_j &= \left(\begin{array}{c} S_{j1}^T M_{B_j}^0 \dot{S}_{j1} - S_{j1}^T \text{ad}_{S_{j2}}^T M_{B_j}^0 S_{j1} \eta_{2j2} - S_{j1}^T M_{B_j}^0 \dot{S}_{j2} - S_{j1}^T \text{ad}_{S_{j2}}^T M_{B_j}^0 S_{j2} \eta_{2j2} \\ S_{j2}^T M_{B_j}^0 \dot{S}_{j1} - S_{j2}^T \text{ad}_{S_{j1}}^T M_{B_j}^0 S_{j1} \eta_{2j1} - S_{j2}^T M_{B_j}^0 \dot{S}_{j2} - S_{j2}^T \text{ad}_{S_{j1}}^T M_{B_j}^0 S_{j2} \eta_{2j1} \end{array} \right) \end{aligned} \quad (79)$$

where $j = 2, 3, 4$.

A suitable choice of positive definite smooth Lyapunov candidate is the total energy of the rigid bodies connected by the passive joints comprising the internal dynamics $V(\eta) : \mathbb{Z} \rightarrow \mathbb{R}_{>0} \forall \eta \neq \eta_e, V(\eta_e) = 0 \forall \eta_e \in \mathbb{D}_{x_e}^{[i]}$

$$V = \frac{1}{2} \eta_2^T \tilde{M}_{tt}(\eta_1 - \eta_{1e}) \eta_2 + \tilde{U}(\eta_1 - \eta_{1e}) \quad (80)$$

where $\tilde{U}(\eta_1 - \eta_{1e})$ is the potential energy of the passive dynamics in the manifold $\eta \in \mathbb{Z}$ whose time derivative is

$$\begin{aligned} \dot{\tilde{U}} &= \eta_2^T \frac{\partial \tilde{U}}{\partial(\eta_1 - \eta_{1e})} \\ &= -\eta_2^T \tilde{S}_t^T(\eta_1 - \eta_{1e}) \text{col}(\tilde{M}_{B_j}(\eta_1 - \eta_{1e}) G^0) = \eta_2^T \tilde{g}_t \end{aligned} \quad (81)$$

where $G^0 = \text{col}(0_5, -9.81 \text{ m/s}^2)$. Taking the time derivatives of V yields

$$\begin{aligned} \dot{V} &= \eta_2^T \tilde{M}_{tt} \dot{\eta}_2 + \frac{1}{2} \eta_2^T \tilde{M}_{tt} \eta_2 + \dot{\tilde{U}} \\ &= \eta_2^T \left(\frac{1}{2} \dot{\tilde{M}}_{tt} - \tilde{C} \right) \eta_2 \\ &\quad - \eta_2^T D_f \eta_2 - \eta_2^T \tilde{g}_t + \eta_2^T D_3 \tilde{z} + \eta_2^T \tilde{g}_t \end{aligned} \quad (82)$$

Since $\frac{1}{2} \dot{\tilde{M}}_{tt} - \tilde{C}$, with $\dot{\tilde{M}}_{tt}$ and \tilde{C} respectively given in Table I and (79), is skew-symmetric, \dot{V} reduces to

$$\dot{V} = -\eta_2^T D_f \eta_2 + \eta_2^T D_3 \tilde{z} \quad (83)$$

Thus for asymptotic stability of η_e , \tilde{z} must satisfy

$$\eta_2^T D_3 \tilde{z} < \eta_2^T D_f \eta_2 \quad (84)$$

Since the quadratic form $\eta_2^T D_f \eta_2$ can be bounded by

$$\lambda_{\min}(D_f) \|\eta_2\|^2 \leq \eta_2^T D_f \eta_2 \leq \lambda_{\max}(D_f) \|\eta_2\|^2$$

Applying Cauchy–Schwarz inequality to bound $|\eta_2^T D_3 \tilde{z}| \leq \|\eta_2\| \|D_3 \tilde{z}\|$ yields the bounds on $\tilde{z} \forall \eta \in \mathbb{Z} - \{\eta_e\}$ to be (19) in original coordinates, where also this norm property $\|D_3 \tilde{z}\| \leq \|D_3\| \|\tilde{z}\|$ is used. The proof is concluded.

D. Proof of Proposition 2

We construct the state feedback $v = \alpha_v(\bar{\zeta})$, with $\bar{\zeta} := (\zeta, x_{11})$, which locally asymptotically stabilizes $\Sigma_{\bar{\zeta}}$ (14), at $\bar{\zeta}_e := (\zeta_e, x_{11e})$. Thus, from Theorem 10.3.1 in [22], the cascaded interconnection of the autonomous system $\Sigma_{\bar{\zeta}}(\bar{\zeta}; \alpha_v(\bar{\zeta}))$ and $\Sigma_\eta(\eta; \bar{\zeta})$ is guaranteed to be LAS in $\mathbb{U}_{\tilde{x}_e} \times SE(3)$ of (\tilde{x}_e, x_{11e}) , given the result in Theorem 1.

Consider the system $\Sigma_3^H(C_1^0; \zeta_1)$ (75). The goal is to find a feedback law for the input ζ_1 to stabilize the equilibrium C_{1e}^0 . To this end, we choose the positive definite smooth Lyapunov

candidate $V_1(C_1^0) : SE(3) \rightarrow \mathbb{R}_{>0}$ $\forall C_1^0 \neq C_{1e}^0$, $V_1(C_{1e}^0) = 0$ to be

$$\begin{aligned} V_1(C_1^0(t)) &= \frac{1}{2} \|C_0^{1e} C_1^0(t) - I\|_F^2 \\ &= \frac{1}{2} \text{tr}((C_0^{1e} C_1^0(t) - I)^T (C_0^{1e} C_1^0(t) - I)) \end{aligned} \quad (85)$$

where $\|\cdot\|_F$ is the Frobenius norm and $\text{tr}(\cdot)$ denotes the trace. The term $C_0^{1e} C_1^0(t)$ is the left-trivialized error on $SE(3)$. Define the variable E_c as

$$E_c = C_0^{1e} C_1^0(t) - I \quad (86)$$

Taking the time derivatives of the $V_1(C_1^0)$ along the trajectories of C_1^0 while simplifying using properties of the trace yields

$$\begin{aligned} \dot{V}_1(C_1^0(t)) &= \frac{1}{2} \frac{d}{dt} \text{tr}(E_c^T E_c) = \frac{1}{2} \text{tr}\left(\frac{d}{dt} E_c^T E_c + E_c^T \frac{d}{dt} E_c\right) \\ &= \frac{1}{2} \text{tr}\left(\frac{d}{dt} E_c^T E_c\right) + \frac{1}{2} \text{tr}(E_c^T \frac{d}{dt} E_c) \\ &= \frac{1}{2} \text{tr}\left(E_c^T \frac{d}{dt} E_c\right)^T + \frac{1}{2} \text{tr}(E_c^T \frac{d}{dt} E_c) \\ &= \text{tr}\left(E_c^T \frac{d}{dt} E_c\right) \end{aligned} \quad (87)$$

Since $\frac{d}{dt} E_c$ is given by

$$\dot{E}_c = C_0^{1e} \frac{d}{dt} C_1^0(t) = C_0^{1e} [\zeta_1] C_1^0(t) \quad (88)$$

Hence

$$\begin{aligned} \dot{V}_1(C_1^0(t)) &= \text{tr}(E_c^T C_0^{1e} [\zeta_1] C_1^0(t)) = \text{tr}(C_1^0(t) E_c^T C_0^{1e} [\zeta_1]) \\ &= \text{tr}(((C_0^{1e})^T E_c (C_1^0)^T)^T [\zeta_1]) \end{aligned} \quad (89)$$

By using the fact that if $b \in se(3)$, $A \in \mathbb{R}^{4 \times 4}$ then this trace property holds $\text{tr}(A^T [b]) = \text{tr}(P_{se(3)}^T(A) [b])$ where $P_{se(3)}(A)$ projects the matrix A on $se(3)$ as follows

$$P_{se(3)}(A) = \begin{pmatrix} \frac{1}{2}(A_{[1:3,1:3]} - A_{[1:3,1:3]}^T) & A_{[1:3,4]} \\ 0_{1 \times 3} & 0 \end{pmatrix} \quad (90)$$

where $A_{[a:b,c,d]}$ constructs a new matrix by extracting from matrix A the rows number a to b and columns number c to d , \dot{V}_1 hence becomes

$$\begin{aligned} \dot{V}_1(C_1^0(t)) &= \text{tr}(P_{se(3)}^T((C_0^{1e})^T E_c (C_1^0)^T)^T [\zeta_1]) \\ &= \hat{P}_{se(3)}^T((C_0^{1e})^T E_c (C_1^0)^T) L \zeta_1 \end{aligned} \quad (91)$$

where $L = \text{diag}(2, 2, 2, 1, 1, 1)$. Now let the input ζ_1 be

$$\zeta_1 = -K_p \hat{P}_{se(3)} \left((C_0^{1e})^T E_c (C_1^0)^T \right) =: \zeta_{1e} \quad (92)$$

where the diagonal gain matrix $K_p > 0 \in \mathbb{R}^{6 \times 6}$ and $\hat{\cdot}$ denotes the inverse map between $se(3) \rightarrow \mathbb{R}^6$. Substituting (92) makes \dot{V}_1 take this quadratic form

$$\begin{aligned} \dot{V}_1(C_1^0(t)) &= -\hat{P}_{se(3)}^T((C_0^{1e})^T E_c (C_1^0)^T) L K_p \hat{P}_{se(3)}((C_0^{1e})^T E_c (C_1^0)^T) \\ &= -\| [K_p^{\frac{1}{2}} \hat{P}_{se(3)}((C_0^{1e})^T E_c (C_1^0)^T)] \|_F^2 < 0 \quad \forall E_c \neq 0 \end{aligned} \quad (93)$$

Now, we follow a backstepping strategy to stabilize the ζ_1 -dynamics at the equilibrium ζ_{1e} (92) using the input ζ_2 . Consider the positive definite smooth Lyapunov candidate

$V_2(C_1^0, \zeta_1) : SE(3) \times se(3) \rightarrow \mathbb{R}_{>0}$, $\forall C_1^0 \neq C_{1e}^0$ and $\forall \zeta_1 \neq \zeta_{1e}$, with $V(C_{1e}^0, \zeta_{1e}) = 0$

$$V_2(C_1^0, \zeta_1) = V_1 + \frac{1}{2} \|\zeta_1 - \zeta_{1e}\|^2 \quad (94)$$

Taking the time derivatives of V_2 gives

$$\dot{V}_2(C_1^0, \zeta_1) = \dot{V}_1 + (\dot{\zeta}_1 - \dot{\zeta}_{1e})^T (\zeta_1 - \zeta_{1e}) \quad (95)$$

hence by substituting the dynamics of ζ_1 (74), i.e., $\dot{\zeta}_1 = \zeta_2$

$$\dot{V}_2(C_1^0, \zeta_1) = \dot{V}_1 + (\zeta_2 - \dot{\zeta}_{1e})^T (\zeta_1 - \zeta_{1e}) \quad (96)$$

and selecting the input ζ_2 as

$$\zeta_2 = \dot{\zeta}_{1e} + \bar{\zeta}_2 \quad (97)$$

thus the derivatives of V_2 reads as

$$\dot{V}_2(C_1^0, \zeta_1) = \dot{V}_1 + \bar{\zeta}_2^T (\zeta_1 - \zeta_{1e}) \quad (98)$$

Setting $\bar{\zeta}_2$ to be $\bar{\zeta}_2 = -K_d(\zeta_1 - \zeta_{1e})$, where the diagonal gain matrix $K_d > 0 \in \mathbb{R}^{6 \times 6}$, renders \dot{V}_2 negative definite $\forall (C_1^0, \zeta_1) \neq (C_{1e}^0, \zeta_{1e})$

$$\dot{V}_2(C_1^0, \zeta_1) = \dot{V}_1 - (\zeta_1 - \zeta_{1e})^T K_d (\zeta_1 - \zeta_{1e}) < 0 \quad (99)$$

The total control law for ζ_2 is

$$\zeta_2 = \dot{\zeta}_{1e} - K_d (\zeta_1 - \zeta_{1e}) =: \zeta_{2e} \quad (100)$$

This step is repeated once again to design a controller v that stabilizes the ζ_2 -dynamics (74) at the equilibrium ζ_{2e} with the Lyapunov candidate $V_3(C_1^0, \zeta_1, \zeta_2)$ given by

$$V_3(C_1^0, \zeta_1, \zeta_2) = V_1(C_1^0) + V_2(C_1^0, \zeta_1) + \frac{1}{2} \|\zeta_2 - \zeta_{2e}\|^2 \quad (101)$$

The equation for the virtual input v is thus obtained as

$$v = \dot{\zeta}_{2e} - K_a (\zeta_2 - \zeta_{2e}) \quad (102)$$

where K_a is a diagonal gain matrix $K_a > 0 \in \mathbb{R}^{6 \times 6}$.

The time derivatives of ζ_{1e} are functions of the first time derivative of the error E_c (86), i.e. \dot{E}_c (88), and

$$\ddot{E}_c = C_0^{1e} \left([\zeta_2] + [\zeta_1]^2 \right) C_1^0 \quad (103)$$

Hence

$$\begin{aligned} \dot{\zeta}_{1e} &= -K_p \hat{P}_{se(3)} \left((C_0^{1e})^T \left(\dot{E}_c (C_1^0)^T + E_c (C_1^0)^T [\zeta_1]^T \right) \right) \\ \dot{\zeta}_{1e} &= -K_p \hat{P}_{se(3)} \left((C_0^{1e})^T \left(\dot{E}_c (C_1^0)^T + 2\dot{E}_c (C_1^0)^T [\zeta_1]^T + E_c (C_1^0)^T (([\zeta_1]^T)^2 + [\zeta_2]^T) \right) \right) \end{aligned} \quad (104)$$

After some algebraic manipulations of (100) and (102), the virtual control v can be rewritten as

$$v = \ddot{\zeta}_{1e} + \bar{K}_d (\dot{\zeta}_{1e} - \zeta_2) + \bar{K}_a (\zeta_{1e} - \zeta_1) \quad (105)$$

where $\bar{K}_a > 0 \in \mathbb{R}^{6 \times 6}$, $\bar{K}_d > 0 \in \mathbb{R}^{6 \times 6}$ are diagonal gain matrices. They are related to K_a and K_d by

$$\bar{K}_a = K_d K_a, \quad \bar{K}_d = K_d + K_a \quad (106)$$

If the error states are defined as

$$e_1(t) := \zeta_{1e} - \zeta_1, \quad e_2(t) := \dot{\zeta}_1 \quad (107)$$

then a linear error system with a state $e = (e_1 \ e_2)^T$ and a pair (A, B) given in Proposition 2 results. The gain matrices \bar{K}_d and \bar{K}_a can thus be tuned to exponentially stabilize its origin by rendering $(A - BK)$ Hurwitz.

Remark 3. *Observe that to eliminate the steady-state error in the convergence of $e(t)$ to zero, which may be present due to parametric uncertainty, an integral term can be added to v as*

$$v = \ddot{\zeta}_{1e} + \bar{K}_d(\dot{\zeta}_{1e} - \zeta_2) + \bar{K}_a(\zeta_{1e} - \zeta_1) + K_I \int (\zeta_{1e} - \zeta_1) dt \quad (108)$$

where $K_I = K_I^T > 0 \in \mathbb{R}^{6 \times 6}$ is the integral gain matrix.

This concludes the proof.

REFERENCES

- [1] M. Sabour, P. Jafary, and S. Nematian, “Applications and classifications of unmanned aerial vehicles: A literature review with focus on multi-rotors,” *The Aeronautical Journal*, vol. 127, no. 1309, pp. 466–490, 2023.
- [2] G. Muscio, F. Pierri, M. A. Trujillo, E. Cataldi, G. Antonelli, F. Caccavale, A. Viguria, S. Chiaverini, and A. Ollero, “Coordinated control of aerial robotic manipulators: Theory and experiments,” *IEEE Transactions on Control Systems Technology*, vol. 26, no. 4, pp. 1406–1413, 2017.
- [3] A. Ollero, M. Tognon, A. Suarez, D. Lee, and A. Franchi, “Past, present, and future of aerial robotic manipulators,” *IEEE Transactions on Robotics*, vol. 38, no. 1, pp. 626–645, 2022.
- [4] M. Tognon, H. A. T. Chávez, E. Gasparin, Q. Sablé, D. Bicego, A. Mallet, M. Lany, G. Santi, B. Revaz, J. Cortés, and A. Franchi, “A truly-redundant aerial manipulator system with application to push-and-slide inspection in industrial plants,” *IEEE Robotics and Automation Letters*, vol. 4, no. 2, pp. 1846–1851, 2019.
- [5] K. Bodie, M. Brunner, M. Pantic, S. Walser, P. Pfändler, U. Angst, R. Siegwart, and J. Nieto, “Active interaction force control for contact-based inspection with a fully actuated aerial vehicle,” *IEEE Transactions on Robotics*, vol. 37, no. 3, pp. 709–722, 2021.
- [6] A. Ali, C. Gabellieri, and A. Franchi, “A control theoretic study on omnidirectional mavs with minimum number of actuators and no internal forces at any orientation,” in *2024 IEEE 63rd Conference on Decision and Control (CDC)*, 2024, pp. 3571–3576.
- [7] R. Rashad, J. Goerres, R. Aarts, J. B. C. Engelen, and S. Stramigioli, “Fully actuated multirotor UAVs: A literature review,” *IEEE Robotics & Automation Magazine*, vol. 27, no. 3, pp. 97–107, 2020.
- [8] M. Hamandi, Q. Sable, M. Tognon, and A. Franchi, “Understanding the omnidirectional capability of a generic multi-rotor aerial vehicle,” in *2021 Aerial Robotic Systems Physically Interacting with the Environment (AIRPHARO)*, 2021, pp. 1–6.
- [9] S. Rajappa, M. Ryll, H. H. Bültlhoff, and A. Franchi, “Modeling, control and design optimization for a fully-actuated hexarotor aerial vehicle with tilted propellers,” in *2015 IEEE International Conference on Robotics and Automation (ICRA)*, 2015, pp. 4006–4013.
- [10] T. D. Howard, C. Molter, C. D. Seely, and J. Yee, “The lynchpin—a novel geometry for modular, tangential, omnidirectional flight,” *SAE International Journal of Aerospace*, vol. 16, no. 3, pp. 291–303, mar 2023. [Online]. Available: <https://doi.org/10.4271/01-16-03-0018>
- [11] S. Park, J. Her, J. Kim, and D. Lee, “Design, modeling and control of omni-directional aerial robot,” in *2016 IEEE/RSJ International Conference on Intelligent Robots and Systems (IROS)*, 2016, pp. 1570–1575.
- [12] M. Hamandi, Q. Sable, M. Tognon, and A. Franchi, “Understanding the omnidirectional capability of a generic multi-rotor aerial vehicle,” in *2021 Aerial Robotic Systems Physically Interacting with the Environment (AIRPHARO)*. IEEE, 2021, pp. 1–6.
- [13] D. Brescianini and R. D’Andrea, “Design, modeling and control of an omni-directional aerial vehicle,” in *2016 IEEE International Conference on Robotics and Automation (ICRA)*, 2016, pp. 3261–3266.
- [14] S. Park, J. Lee, J. Ahn, M. Kim, J. Her, G.-H. Yang, and D. Lee, “Odar: Aerial manipulation platform enabling omnidirectional wrench generation,” *IEEE/ASME Transactions on mechatronics*, vol. 23, no. 4, pp. 1907–1918, 2018.
- [15] M. Ryll, H. H. Bültlhoff, and P. R. Giordano, “A novel overactuated quadrotor unmanned aerial vehicle: Modeling, control, and experimental validation,” *IEEE Transactions on Control Systems Technology*, vol. 23, no. 2, pp. 540–556, 2014.
- [16] A. Oosedo, S. Abiko, S. Narasaki, A. Kuno, A. Konno, and M. Uchiyama, “Flight control systems of a quad tilt rotor unmanned aerial vehicle for a large attitude change,” in *2015 IEEE International Conference on Robotics and Automation (ICRA)*, 2015, pp. 2326–2331.
- [17] M. Kamel, S. Verling, O. Elkhatib, C. Sprecher, P. Wulkop, Z. Taylor, R. Siegwart, and I. Gilitschenski, “The voliro omniorientational hexacopter: An agile and maneuverable tilttable-rotor aerial vehicle,” *IEEE Robotics & Automation Magazine*, vol. 25, no. 4, pp. 34–44, 2018.
- [18] M. Zhao, T. Anzai, F. Shi, X. Chen, K. Okada, and M. Inaba, “Design, modeling, and control of an aerial robot dragon: A dual-rotor-embedded multilink robot with the ability of multi-degree-of-freedom aerial transformation,” *IEEE Robotics and Automation Letters*, vol. 3, no. 2, pp. 1176–1183, 2018.
- [19] M. Ryll, D. Bicego, and A. Franchi, “Modeling and control of fast-hex: A fully-actuated by synchronized-tilting hexarotor,” in *2016 IEEE/RSJ International Conference on Intelligent Robots and Systems (IROS)*, 2016, pp. 1689–1694.
- [20] Y. Abdourra, C. Gabellieri, R. Brantjes, Q. Sablé, and A. Franchi, “Modelling, analysis, and control of omnimorph: an omnidirectional morphing multi-rotor uav,” *Journal of Intelligent & Robotic Systems*, vol. 110, no. 1, p. 21, 2024.
- [21] M. Hamandi, F. Usai, Q. Sable, N. Staub, M. Tognon, and A. Franchi, “Design of multirotor aerial vehicles: a taxonomy based on input allocation,” *The International Journal of Robotics Research*, vol. 40, no. 8-9, pp. 1015–1044, 2021.
- [22] A. Isidori, *Nonlinear Control Systems II*, ser. Communications and Control Engineering. Springer London, 1999. [Online]. Available: <https://link.springer.com/book/10.1007/978-1-4471-0549-7>
- [23] J. Descusse and C. Moog, “Dynamic decoupling for right-invertible nonlinear systems,” *Systems & Control Letters*, vol. 8, no. 4, pp. 345–349, 1987. [Online]. Available: <https://www.sciencedirect.com/science/article/pii/0167691187901010>
- [24] R. Featherstone, *Rigid body dynamics algorithms*. Springer, 2014.
- [25] R. M. Murray, Z. Li, and S. S. Sastry, *A mathematical introduction to robotic manipulation*. CRC press, 2017.
- [26] A. Isidori, *Nonlinear Control Systems*, ser. Communications and Control Engineering. Springer London, 2013. [Online]. Available: <https://books.google.it/books?id=N9h5BgAAQBAJ>
- [27] M. Spong, “Partial feedback linearization of underactuated mechanical systems,” in *Proceedings of IEEE/RSJ International Conference on Intelligent Robots and Systems (IROS’94)*, vol. 1, 1994, pp. 314–321 vol.1.